



**QUEEN'S  
UNIVERSITY  
BELFAST**

## **Holocene establishment of mangrove forests in the western coast of the Gulf of Mexico**

Cordero-Oviedo, C., Correa-Metrio, A., Urrego, L. E., Vázquez-Hurtado, G., Blaauw, M., Escobar, J., & Curtis, J. H. (2019). Holocene establishment of mangrove forests in the western coast of the Gulf of Mexico. *CATENA*, 180, 212-223. <https://doi.org/10.1016/j.catena.2019.04.025>

**Published in:**  
CATENA

**Document Version:**  
Peer reviewed version

**Queen's University Belfast - Research Portal:**  
[Link to publication record in Queen's University Belfast Research Portal](#)

### **Publisher rights**

Copyright 2019 Elsevier.

This manuscript is distributed under a Creative Commons Attribution-NonCommercial-NoDerivs License

(<https://creativecommons.org/licenses/by-nc-nd/4.0/>), which permits distribution and reproduction for non-commercial purposes, provided the author and source are cited.

### **General rights**

Copyright for the publications made accessible via the Queen's University Belfast Research Portal is retained by the author(s) and / or other copyright owners and it is a condition of accessing these publications that users recognise and abide by the legal requirements associated with these rights.

### **Take down policy**

The Research Portal is Queen's institutional repository that provides access to Queen's research output. Every effort has been made to ensure that content in the Research Portal does not infringe any person's rights, or applicable UK laws. If you discover content in the Research Portal that you believe breaches copyright or violates any law, please contact [openaccess@qub.ac.uk](mailto:openaccess@qub.ac.uk).

### **Open Access**

This research has been made openly available by Queen's academics and its Open Research team. We would love to hear how access to this research benefits you. – Share your feedback with us: <http://go.qub.ac.uk/oa-feedback>

Manuscript Number: CATENA7971R1

Title: Holocene establishment of mangrove forests in the western coast of the Gulf of Mexico

Article Type: Research Paper

Keywords: coastal environment; Gulf of Mexico; Holocene; mangroves; sea-level changes; pollen analysis

Corresponding Author: Dr. Alexander Correa-Metrio,

Corresponding Author's Institution:

First Author: Cecilia Cordero-Oviedo

Order of Authors: Cecilia Cordero-Oviedo; Alexander Correa-Metrio; Ligia Estela Urrego; Gabriela Vázquez-Hurtado; Maarten Blaauw; Jaime Esconar; Jason Curtis

Abstract: The successful establishment of mangrove ecosystems depends on an intricate network of interactions among physical and biological factors that are highly dynamic through time. At millennial to centennial time scales, regional climates, sea levels, and local geomorphology play critical roles in the establishment of mangroves. Whereas fluvio-marine dynamics define coastal sedimentary settings, regional precipitation and freshwater input modulate salinity and seasonal flooding patterns. We analyzed a ~7800-year-old, continuous sedimentary record from the western coast of the Gulf of Mexico to shed light on regional biophysical coastal processes and the history of the mangroves that occupy the region today. We used a systematic sampling of mud-water interface sediments to generate a modern reference frame for interpreting fossil pollen assemblages. Our results indicate that the cored location that is currently approximately at sea level, was below sea level from ~7800 to 4000 calibrated years before present (cal BP). The establishment of dense mangrove stands took place around 3700 cal BP, when regional sea levels stabilized, resulting in a substantial increase of organic matter and therefore carbon stored in the sediments. However, the mangrove ecological succession that started at ~6000 cal BP was interrupted by a regional drought that extended from ~5400 to 3700 cal BP. From 3700 cal BP to Present, the lagoon has been characterized by relatively stable both substratum and sea level, that together have facilitated the establishment of mangrove forests. Overall, our record demonstrates the complexity of the interactions between local and regional factors in the development and evolution of both coastal geomorphology and ecosystems.

Dear Dr. Cammeraat

We are happy to submit a revised version of the manuscript entitled “Holocene establishment of mangrove forests in the western coast of the Gulf of Mexico”. We are very appreciative of the thorough review of the manuscript because it substantially improved it. The main change we made was including carbon and nitrogen analyses on both modern and fossil samples, giving more solid bases to our interpretations. We have included Jason Curtis and Jaime Escobar as coauthors because they very kindly contributed the C and N analysis and helped with the interpretation of results. Please find below the response to the queries from the reviewer, whereas the idiomatic suggestions marked on the pdf were directly attended on the word documents, which marked up copy we are attaching too. Please extend all our gratitude to the reviewer, he did a fantastic job at raising conceptual and stylistic concerns.

We feel that the new version is much better and stronger, we hope you find it suitable for publications in CATENA.

Sincerely yours,

Alex Correa-Metrio

**Reviewer #1: This paper provides a reconstruction of change in the La Mancha lagoon, on Mexico's east coast, based on pollen analysis. In fact, it relies almost entirely on pollen, with only a passing reference to stratigraphy. As the authors themselves note, the evolution of these coastal systems involves the complex interplay of a number of factors, a challenge that really needs a multi-proxy approach. There are some hints that there might be some other information available, but it is not presented (see below).**

We are aware of the importance of a multiproxy approach, and thus, we have decided to add analyses of total both carbon and nitrogen in modern and fossil samples. The inclusion of new data has strengthened our case, but we, however, would like to emphasize that the aim of our research, as clearly stated in the manuscript, is reconstructing vegetation dynamics, a goal that is achieved through pollen analysis. Mangrove forests develop under a precise combination of geomorphologic settings as well as fluvial and marine influences, thus the use of mangrove pollen has been recognized as a reliable and efficient means for reconstructing environmental dynamics in coastal environments.

**The water level reconstructions in particular seem really quite speculative based on pollen alone and the lack of information about the morphology of the modern lagoon.**

We have added a basic bathymetry based on data points that were measured during the collection of modern samples.

**There are a number of places where more detail is needed and more justification for some of the reconstructions made. This need for clearer justification feeds through to the Highlights listed. Although the quality of the English was generally good, there were a few places where the meaning was not clear (see annotated pdf uploaded).**

The document was changed according to the comments on the pdf.

**Study area. More about the morphology of lagoon (is there anything in Reassert, 1999?) would be useful.**

We included a basic bathymetry. Also, in Section 2 (Study area), we abounded “La Mancha lagoon belongs to a geomorphic unit known as the Low Cumulative Plain that formed during the Quaternary (Geissert, 1999), allowing deposition of clayey-silt sediments. The lagoon formed at the margin of a volcanic mountain range that interrupts the coastal plain of the Gulf of Mexico (Geissert, 1999; Fig. 1). The current morphology of the area has been mostly shaped by Quaternary dynamics, going from an empty deep basin during times of sea-level low stands to a depositional coastal plain during times of sea-level high stands (Geissert, 1999; Kjerfve, 1994). The mountain ridge that connects La Mancha Hill with the adjacent western mountains divides La Mancha lagoon into two contrasting sub-basins (Fig. 1). Differences in freshwater input, marine influence, energy of the sedimentary environments, and human occupation have created two clearly distinct environments for mangrove forests, which today occupy ~3.55 km<sup>2</sup> around the lagoon”

**What was transect in Fig. 1 based on?**

The transect represented an arbitrary line that was drawn aiming to describe the morphology and likely evolution of the area. We have excluded the transect and replaced Fig. 1D.

**More detail is needed here about canals (referred to later) and the nature and extent of human impact.**

There was an idiomatic misunderstanding, we misused the word “canals” for referring to drainage channels. We have amended the text likewise. Also, we have reworded the last paragraph of Study Area, which now reads “Regional human occupation has been reported since at least ~4,600 BP, and the lagoon has apparently been an important source of resources for human populations (Moreno-Casasola, 2006). This factor has exerted direct pressure on the mangrove forest through deforestation for timber and fuel wood extraction, and more recently in the interruption of surface and subsurface flows in the by infrastructure of the oil industry. These local factors have been especially harsh on the northern sub-basin, where only sparse remnants of the mangrove forest survive today. Thus, whereas vigorous mangrove forests surround the southern sub-basin, the northern sub-basin is occupied by highly disturbed vegetation including sparse mangrove remnants. Regionally, growing human population and the parallel development of infrastructure apply further pressures to coastal ecosystems through pollution, accelerated erosion, increasing sea level, among other elements (Gilman et al., 2008).”

**Methods. Were water depths measured when the surface sediment samples were taken?**

Yes, we have added a bathymetric map of the lagoon.

**Did you measure LOI for these samples to look at spatial variability? Grain size? This information would give an idea of basin bathymetry. Presumably there would be a clear river channel?**

We added analyses of TIC, TOC, and TN on surface samples and demonstrated that there are significant differences between the northern and southern sub-basins, providing further, more solid elements for interpreting the fossil record “TC content in modern samples varied between 3.1 and 12.3%, with mean and median of 4.9 and 4.4%, respectively. Although mean values for the northern and southern sub-basins were not statistically differentiable ( $t = 1.66$ ,  $p\text{-value} = 0.11$ ), the northern sub-basin consistently showed lower values (Fig. 3). Differently, individual fractions of C resulted statistically differentiable, with a higher concentration of TOC in the southern sub-basin ( $3.56$ ,  $p\text{-value} = 0.002$ ) and a higher concentration of TIC in the northern sub-basin ( $t = -2.47$ ,  $p\text{-value} = 0.023$ ). TN range between 0.02 and 0.37% with mean and median of 0.23 and 0.24%, respectively (Fig. 3), with southern concentration statistically higher than the northern concentration ( $t = 5.54$ ,  $p\text{-value} < 0.001$ ). TC resulted statistically associated with TN, TIC, and TOC, although the magnitude of the correlation was substantially higher with the latter (Fig. 3). Whereas TIC resulted moderately associated only with TN, TOC was strongly associated with both TC and TN (Fig. 3).”

**What evidence do you have to support claim of deep and bucket shape basin?**

Where it read “Thus, the lacustrine basin of La Mancha was probably deep and bucket-shaped, impeding the establishment of mangrove forests”, it now reads “Thus, the lacustrine basin of La Mancha was probably deeper than modern, impeding the establishment of mangrove forests”.

**Was anything else done on the core other than pollen? LOI? What were the shells, terrestrial? aquatic/ freshwater or marine? Do they tell you anything directly about salinity?**

We have added TC and TN analyzed on modern and fossil samples, which greatly strengthened our interpretation. Biological indicators other than pollen provide a wealth of information on different environmental attributes. The goal of our research was reconstructing the evolution of the mangrove forest, which we did through the fossil pollen record, and the modern context provided by the spatial sampling. The shells we found were marine bivalves, and we then clarified in the discussion that their presence through the record evidences a constant marine influence through time. We added to the discussion “Additionally, the constant presence of marine shells through the sedimentary record (Fig. 2) demonstrates a permanent marine influence through the last ~7,800 year.”

**Results. Radiocarbon dates - need to add calibrated dates to Table 1.**

Calibrated dates were added to Table 1.

**Why bulk dates? What was OM content? See query above re LOI.**

The material dated was bulk sediment since no other material such as macrofossils or charcoal could be found. We are aware of the possibility of a  $^{14}\text{C}$  age offset but were not able to quantify this in the present study. We added TC and TN for the entire record,

making evident that the content of TC of points sampled for radiocarbon analyses varied between 2 and 7%. Although TC content is likely associated with the organic fraction, we did not quantify organic matter content for the fossil samples.

**Add actual dates to Fig 2.**

Actual dates are in Table 1, thus we considered it was not necessary repeating this information on Fig. 2 as the figure is already crowded.

**What was/is human disturbance in N basin? When did it start? (see above).**

In the study area it now reads “Regional human occupation has been reported since at least ~4,600 BP, and the lagoon has apparently been an important source of resources for human populations (Moreno-Casasola, 2006). This factor has exerted direct pressure on the mangrove forest through deforestation for timber and fuel wood extraction, and more recently in the interruption of surface and subsurface flows in the by infrastructure of the oil industry. These local factors have been especially harsh on the northern sub-basin, where only sparse remnants of the mangrove forest survive today. Thus, whereas vigorous mangrove forests surround the southern sub-basin, the northern sub-basin is occupied by highly disturbed vegetation including sparse mangrove remnants. Regionally, growing human population and the parallel development of infrastructure apply further pressures to coastal ecosystems through pollution, accelerated erosion, increasing sea level, among other elements (Gilman et al., 2008).”

**Was NMDS run on core samples alone to improve discrimination between these?**

No; as stated in the text, NMDS was run on both modern and fossil samples as our interest was to investigate the establishment of modern systems in the area.

**Discussion. More about the % mangrove taxa in the surface sediment and core samples compared to modern % vegetation cover would be useful.**

We don't have reliable quantitative data on the forest surrounding La Mancha. We discuss mangrove representation in the first two paragraphs of the discussion, where we demonstrate that although mangrove taxa percentages are generally high, there is a clear distinction of percentages between the two sub-basins.

**Base of core - sea water flooding - text indicates this recorded at 12-13m below modern surface. How far below modern was sea level 8 - 6 Ka? Is it 6m (see bottom of p.23)? Is there any other evidence to support the idea of sea-water flooding and then a deep water body? (see above).**

See level regional curves for the Gulf of Mexico and the Caribbean are shown in Fig. 7 (former Fig. 6), and their difference with sediment depth were used for estimating lagoon water depth. We explained better in the discussion that now reads “Through this time period, the mud-water interface was between 13 and 9 m below the modern surface, which today is at sea level. At the same time, average sea level was between 9 and 5 m below modern. The difference between mud-water interface depth and sea level can only be accounted by lagoon water depth, which was ~ 4 m below sea level (Fig. 6A).”

**On Fig. 6 do the depths on the y axis relate to both core depth and the height of sea level relative to modern?**

Fig. 7 (former Fig. 6) is meant to compare the depth and age scales of core depth and sea level, and thus they have to necessarily be the same. To avoid confusion, the y-axis label that read “Depth (m)”, now reads “Depth (m below modern surface)”.

**6300-5400 Is there any clear evidence to support the claim of complete closure of the lagoon? Period of more silt deposition. Are these sediments more organic?**

We tried to clarify through the manuscript that the establishment of mangroves (either true mangrove trees or marshland vegetation) requires depositional environments, which an open lagoon would not have provided given the high energy of direct sea influence. We hope to have strengthened our interpretation by adding the curves of TC and TN.

**5400-3700 What's the real basis for identifying modern seasonal cycle?**

This is just an interpretation based on the fact that sea level and sediment interface level apparently became similar. We explained better in the text that now reads “Whereas the rate of sea-level rise continued to decrease, relatively high sedimentation rates were evident in La Mancha sequence up to ~5000 cal BP, when apparently the rates of sediment deposition in the lagoon and those of sea level rise became similar (Fig. 6A). Such equilibrium between sediment deposition and sea-level rise implies the definition of a coastal erosive baseline that allowed the deposition of sand in the coast by the northerly currents during the dry season, creating the sandbar that dams the lagoon. Differently, during the wet season, the fluvial input would have the capacity to erode the sandbar, opening the direct contact between the lagoon and the sea and, thus, resulting in the modern seasonal flood cycle.”

**Last 3700 what's the balance between climate, sea level and human disturbance? See note above re what is known about disturbance?**

I hope this question has been addressed by the multiple changes we made through the document.

1 **Holocene establishment of mangrove forests in the western coast of the Gulf of Mexico**

2

3 Cordero-Oviedo, C<sup>a</sup>., A. Correa-Metrio<sup>b,\*</sup>, L.E. Urrego<sup>c</sup>, G. Vázquez-Hurtado<sup>d</sup>, M.

4 Blaauw<sup>e</sup>, [J. Escobar<sup>f,g</sup>](#), [J.H. Curtis<sup>h</sup>](#)

5 <sup>a</sup> Posgrado en Ciencias de la Tierra, Universidad Nacional Autónoma de México,  
6 Coyoacán, Ciudad de México, México 04510, [ceciliacorderoviedo@gmail.com](mailto:ceciliacorderoviedo@gmail.com), <sup>b</sup>  
7 Instituto de Geología, Universidad Nacional Autónoma de México, Coyoacán,  
8 Ciudad de México, México 04510, [acorrea@geologia.unam.mx](mailto:acorrea@geologia.unam.mx), <sup>c</sup> Departamento de  
9 Ciencias Forestales, Universidad Nacional de Colombia, Sede Medellín A.A. 568  
10 Medellín, Colombia, [leurrego@unal.edu.co](mailto:leurrego@unal.edu.co), <sup>d</sup> Instituto de Ecología, A.C. Carretera  
11 antigua a Coatepec 351, El Haya, Xalapa 91070, Veracruz, México,  
12 [gabriela.vazquez@inecol.mx](mailto:gabriela.vazquez@inecol.mx), <sup>e</sup> School of Natural and Built Environment, Queen's  
13 University Belfast, Belfast, United Kingdom, [maarten.blaauw@qub.ac.uk](mailto:maarten.blaauw@qub.ac.uk), <sup>f</sup>  
14 [Departamento de Ingeniería Civil y Ambiental, Universidad del Norte, Km 5 Via Puerto](#)  
15 [Colombia, Colombia, \[jescobar@uninorte.edu.co\]\(mailto:jescobar@uninorte.edu.co\), <sup>g</sup> Center for Tropical Paleocology and](#)  
16 [Archaeology, Smithsonian Tropical Research Institute, Box 0843-03092, Balboa, Panama,](#) <sup>h</sup>  
17 [Department of Geological Sciences, University of Florida, Gainesville, FL, 32611, USA,](#)  
18 [curtisj@ufl.edu](mailto:curtisj@ufl.edu)

19

20 **\*Corresponding autor:** Alexander Correa-Metrio, [acorrea@geologia.unam.mx](mailto:acorrea@geologia.unam.mx)

21

22 **Abstract**

23 The successful establishment of mangrove ecosystems depends on an intricate network of  
24 interactions among physical and biological factors that are highly dynamic through time. At  
25 millennial to centennial time scales, regional climates, sea levels, and local geomorphology



26 play critical roles in the establishment of mangroves. Whereas fluvio-marine dynamics  
27 define coastal sedimentary settings, regional precipitation and freshwater input modulate  
28 salinity and seasonal flooding patterns. We analyzed a ~7800-year-old, continuous  
29 sedimentary record from the western coast of the Gulf of Mexico to shed light on regional  
30 biophysical coastal processes and the history of the mangroves that occupy the region  
31 today. We used a systematic sampling of mud-water interface sediments to generate a  
32 modern reference frame for interpreting fossil pollen assemblages. Our results indicate that  
33 the cored location that is currently approximately at sea level, was ~~under~~ below sea level  
34 from ~7800 to 4000 calibrated years before present (cal BP). The establishment of dense  
35 mangrove stands took place around 3700 cal BP, when regional sea levels stabilized,  
36 resulting in a substantial increase of organic matter and therefore carbon stored in the  
37 sediments. However, the mangrove ecological succession that started at ~6000 cal BP was  
38 interrupted by a regional drought that extended from ~5400 to 3700 cal BP. From 3700 cal  
39 BP to Present, the lagoon has been characterized by relatively stable both substratum and  
40 sea level, that together have facilitated the establishment of mangrove forests. Overall, our  
41 record demonstrates the complexity of the interactions between local and regional factors in  
42 the development and evolution of both coastal geomorphology and ecosystems.

43

44 Keywords: coastal environment; Gulf of Mexico; Holocene; ~~pollen analysis~~ mangroves;  
45 sea-level changes; pollen analysis

46

## 47 **1. Introduction**

48 Mangrove ecosystems are a large component of tropical and sub-tropical coastal  
49 landscapes. Occupying intertidal zones (Lugo and Snedaker, 1974), they intermediate  
50 regulate the relationship between continental ~~discharges~~discharge of sediments and water;  
51 ~~mainly fluvial,~~ and sea level (Ellison, 1989). The main engineers of these ecosystems are a  
52 reduced group of plant species physiologically adapted to brackish-to-saline substrates  
53 (Ball, 2002; Vovides et al., 2014). The establishment of mangrove forests creates the  
54 conditions for complex food webs that incorporate marine and continental components. The  
55 entire mangrove ecosystem is fundamental for providing products and ecological services,  
56 ~~which reflect~~resulting in direct and indirect uses by human populations, mainly fuelwood,  
57 fisheries, sediment trapping, and carbon storage (Bouillon et al., 2008; Feller et al., 2017;  
58 Méndez et al., 2007; Ward et al., 2016).

59 Although they represent one of the most important carbon sinks worldwide  
60 (Bouillon et al., 2008), together with coral reefs and tropical forests, mangroves are among  
61 the most endangered modern ecosystems (Valiela et al., 2001). It has been estimated that  
62 through the last two decades of the 20th Century, 35% of the global mangrove area had  
63 been lost mostly because of direct and/or indirect anthropogenic causes (FAO, 2007). The  
64 main human-related causes of mangroves loss are the conversion to aquaculture and  
65 agriculture, urbanization, and pollution (Feller et al., 2017; Gilman et al., 2008; Thorhauga  
66 et al., 2017), which in Mexico have translated in a net loss ~240 ha/year through the last  
67 decades (Hamilton and Cassey, 2016). The rapid rate at which these threats to mangrove  
68 ecosystems are growing highlights the need ~~of to~~understanding them in the context of their  
69 natural history and the intricate network of factors that interact to facilitate or impede their  
70 colonization and establishment.

71 A wide variety of factors interact to create the specific conditions under which  
72 mangrove communities thrive and persist through time (Gilman et al., 2008). Healthy  
73 vigorous mangrove forests, and therefore ecosystems, depend on a delicate balance  
74 between marine influences and freshwater and sediment input from continental areas acting  
75 upon specific geomorphologic settings (~~Chapman, 1976~~; Lugo and Snedaker, 1974; Soares,  
76 2009). Whereas marine influences on mangrove ecosystems materialize through tidal  
77 regimes and sea level changes that define base-levels for erosion and accumulation of  
78 sediments, regional climates and vegetation cover over the mainland control continental  
79 discharge of freshwater and sediments along the coast. Thus, through the Holocene,  
80 changes in precipitation, vegetation cover, geomorphologic dynamics, and sea levels have  
81 probably led to high environmental variability over the intertidal areas (Geissert [Kientz](#),  
82 1999). In the Gulf of Mexico and the Caribbean, regional sea levels have progressively  
83 risen since the deglaciation (Milliken and Anderson, 2008; Toscano and Macintyre, 2003),  
84 whereas annual precipitation has shown a wide variability associated with extraterrestrial  
85 forcings (e.g. solar activity and orbital cycles, Haug et al. 2001, Hodell et al. 2001) and  
86 higher frequency processes associated with complex internal systems (e.g. El Niño-  
87 Southern Oscillation, Moy et al. 2002). The balance between fluvial loads and sea-level rise  
88 modulates local geomorphologic and sedimentary processes, defining the formation of  
89 either depositional or erosional environments [the balance of](#) which ~~balance~~ is in turn critical  
90 for the establishment and persistence of mangroves (Parkinson et al., 1994). Indeed,  
91 modern net losses of mangrove cover have been widely associated with sea-level rises  
92 along unprotected coasts (Suárez et al., 2015). Thus, the definition of the context that led to  
93 the development of modern mangrove forests would provide important clues for identifying  
94 the limits of environmental pressure that these ecosystems can endure.

95 Sedimentary deposits that accumulate in coastal lagoons provide a natural record of  
96 the evolution of coastal landscapes through time. Understanding the natural development of  
97 mangrove ecosystems and the main factors involved in the process would give insights into  
98 the threat level that coastal zones face given modern environmental change (Lopez-Portillo  
99 et al., 2011; Thom, 1967). Here we use the pollen record of a 13-m-long ~8,000-year-old  
100 sedimentary sequence retrieved from La Mancha Lagoon, State of Veracruz, Mexico, to  
101 reconstruct the history of the local vegetation through the Holocene. By analyzing the  
102 history of vegetation assemblages as reflected by fossil pollen spectra, we aim to answer  
103 the following questions: i) what has been the role of sea-level rise and precipitation  
104 variability through the Holocene in the establishment and persistence of mangrove forests  
105 in the west coastline of the Gulf of Mexico? ii) when did the barrier-lagoon systems of the  
106 region consolidate in the context of Holocene environmental variability?

107

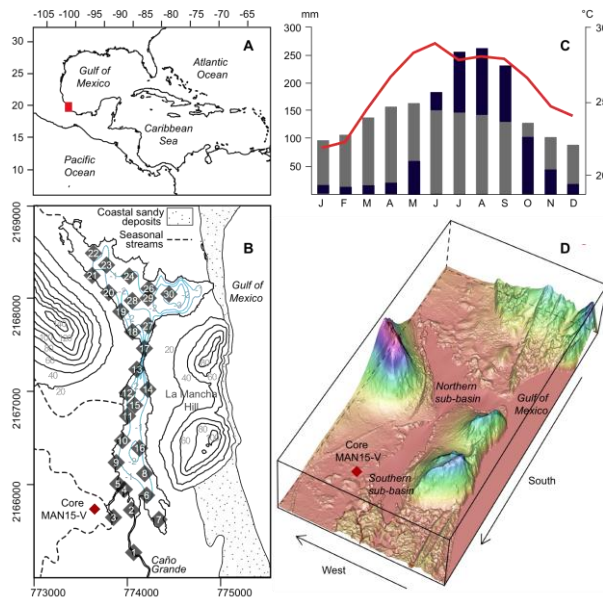
## 108 2. Study Area

109 La Mancha lagoon is located in the State of Veracruz, Mexico, on the western  
110 coasts of the Gulf of Mexico (19.579 N°, 96.387 W°, Fig. 1). With a north-to-south length  
111 of 3 km, the lagoon has an area of ~1.35 km<sup>2</sup> distributed in two sub-basins separated by a  
112 strait located around-near the center of the water body (Fig. 1). Whereas the southern sub-  
113 basin is exposed to permanent freshwater input from the Caño Grande River that drains  
114 water from a basin of almost 2,500 km<sup>2</sup>, the northern sub-basin more exposed to tidal  
115 influence through an ephemeral mouth that communicates seasonally with the sea  
116 seasonally (Fig.1) (Lankford, 1977; Moreno-Casasola, 2006). During the dry season, a sand  
117 bar accumulates closing the estuarine mouth and causing a damming of continental

118 freshwater. With the onset of the rainy season, freshwater starts to accumulate, eventually  
119 breaking the sandbar, opening the mouth, and creating a direct connection with the sea  
120 (Moreno-Casasola, 2006). Thus, lagoon dynamics are intimately linked to regional climate  
121 that is warm (temperatures from 22 to 26 °C), with an annual mean precipitation of 1222  
122 mm, with 85% of the annual value falling between June and October (Fig. 1) (Servicio  
123 Meteorológico Nacional, 2018). The dry season is especially pronounced between  
124 December and April with mean monthly precipitations below 20 mm, ~~whereas~~ while  
125 November and May are characterized by a mean precipitation around 50 mm. By the end of  
126 the summer and early autumn, the area is exposed to tropical cyclones, although their  
127 incidence is relatively low compared with other areas of the Gulf of Mexico (Moreno-  
128 Casasola, 2006).

129 La Mancha lagoon belongs to a geomorphic unit known as the Low Cumulative  
130 Plain that formed during the Quaternary (Geissert Kientz, 1999), allowing deposition of  
131 clayey-silt sediments. The lagoon formed at the margin of a volcanic mountain range that  
132 interrupts the coastal plain of the Gulf of Mexico (Geissert Kientz, 1999; Fig. 1). The  
133 current morphology of the area has been mostly shaped by Quaternary dynamics, going  
134 from an empty deep basin during times of sea-level low stands to a depositional coastal  
135 plain during times of sea-level high stands (Geissert Kientz, 1999; Kjerfve, 1994). The  
136 mountain ridge that connects La Mancha Hill with the adjacent western mountains divides  
137 La Mancha lagoon into two contrasting sub-basins (Fig. 1). The lagoon formed at the  
138 margin of a volcanic mountain range that interrupts the coastal plain of the Gulf of Mexico  
139 (Geissert, 1999) (Fig. 1). Differences in freshwater input, marine influence, and energy of  
140 the sedimentary environments have created two clearly distinct environments for mangrove  
141 forests, which today occupy ~3.55 km<sup>2</sup> around the lagoon.

142 Regional tides are mixed, mostly diurnal and of low amplitude (highest and lowest  
 143 tidal levels at 22 cm and -30 cm from average sea level, respectively), preventing the  
 144 formation of tidal currents. This feature together with the permanent input of fresh water  
 145 and the sheltering of the lagoon from the energy of the waves by La Mancha Hill (Fig. 1)  
 146 have probably played a critical role at-in maintaining the morphology of the lagoon,  
 147 avoiding the formation of tidal coasts mudflats, marshes, and/or estuaries (Geissert [Kientz,](#)  
 148 1999). Through the last Over recent decades, progressive loss of depth of the lagoon  
 149 because of sediment accumulation suggests that sediment input surpasses local erosion  
 150 ([Matus-Moreno-Casasola et al., 1994](#) [2006](#)), although this might not have been the case  
 151 through the entire history of the area.



152  
 153 Figure 1. Study area. A. Location of La Mancha lagoon in the continental context. B.  
 154 Locations sampled for modern and fossil sediments in the local context of La Mancha

155 | coastal lagoon; elevation contours are shown in increments of 20 m asl (solid black lines),  
156 | whereas a basic bathymetry based on field observations is shown as blue contours. C.  
157 | Monthly precipitation (blue bars), evapotranspiration (gray bars), and monthly mean  
158 | temperature (black line with dots) at La Mancha Meteorological Station (Servicio  
159 | Meteorologico Nacional, 2018) D. Topographic ~~profile through~~representation of La  
160 | Mancha coastal lagoon.

161

162 | Pollen assemblages contained in sediments reflect parental vegetation and are  
163 | therefore useful for reconstructing environmental dynamics through time (e.g. Carrillo-  
164 | Bastos et al., 2010; Urrego et al., 2009; Urrego et al., 2018). Given the regional  
165 | geomorphology, the large size of the catchment basin of Caño Grande River, and the  
166 | proximity to high mountain ranges, the pollen spectra of sediments from La Mancha lagoon  
167 | ~~might contains~~ regional and local taxa (Moreno-Casasola, 2006; Travieso-Bello, 2000).  
168 | Whereas the former are transported by water and wind currents, the latter are produced by  
169 | *in situ* vegetation (Hooghiemstra et al., 2006). Regional elements come mostly from  
170 | montane forests that dominate the regional highlands (Rzedowski, 2006~~García Franco et al.,~~  
171 | ~~2008~~; Williams-Linera, 2002) and are characterized by wind-pollinated anemophyllous taxa  
172 | with long-distance pollen dispersal (e.g. *Alnus*, *Myrica*, Ulmaceae, *Quercus*, and *Pinus*),  
173 | which ~~in turn result~~ tend to be overrepresented in the pollen spectra. From within these  
174 | allochthonous elements, *Pinus* is worth noticing because of the opportunist nature of most  
175 | of the parental species (Richardson, 1998), which results in a high representation of this  
176 | taxon in pollen ~~sepectra~~ when environmental conditions are suboptimal for other arboreal  
177 | elements (e.g. during droughts, Correa-Metrio et al., 2013). Local elements of the pollen  
178 | spectra are ~~a~~ in turn associated with two main vegetation types, namely lowland and

Formatted: English (United States)

179 mangrove forests. The hills that surround the lagoon reach heights up to 300 m asl and are  
180 mostly occupied by species of *Desmodium*, *Inga*, *Machaerium*, *Psychotria*, *Protium*,  
181 *Bursera*, Moraceae-Urticaceae and *Acacia*. The salt marshes, coastal dunes, and beaches  
182 that characterize ~~local-cumulative~~flood plains are mainly dominated by species of  
183 Cyperaceae, Amaranthaceae, *Typha*, Asteraceae, Chenopodiaceae, *Mimosa* and *Croton*.  
184 These vegetation types can be associated with the distal part of a marine transgression  
185 plaine, or be related to the first stage of a progradational pattern indicative of a typical  
186 ecological succession on intertidal habitats (González and Dupont, 2009).

187 The edges of the lagoon are occupied by species typical of mangrove forests,  
188 *Rhizophora mangle*, *Avicennia germinans*, *Conocarpus erectus* and *Laguncularia*  
189 *racemosa* (Travieso-Bello, ~~2000~~and Moreno-Casasola, 2006). The interplay of these  
190 species is modulated by their differential adaptation to the changing environmental  
191 conditions along a salinity gradient, which in turn defines the structure and composition of  
192 the forest (Lugo and Snedaker, 1974; Travieso-Bello, 2000; Urrego et al., 2009). Thus,  
193 these forests are highly sensitive to changes in sea-level, coastal progradation and/or  
194 erosion at different time scales (Ellison, 2008). Mangrove forest species are adapted to  
195 specific environmental conditions, with *R. mangle* tolerating high inundation levels, strong  
196 wave energy and shorter distances to the sea, *A. germinans* thriving in more saline  
197 environments, hurricane-disturbed or experiencing severe droughts, *L. racemosa* ~~is-being~~  
198 restricted to average minimum temperatures ~~of more than~~over 15.5 °C and successional  
199 processes triggered by anthropogenic disturbance, and *C. erectus* being tolerant to higher  
200 sediment pH typical of supra-tidal waters close to well drained forests (González et al.,  
201 2010; Hogarth, 2007; Urrego et al., 2009; Urrego et al., 2010).



202 Regional human occupation has been reported since at least ~4,600 BP, and the  
203 lagoon has apparently been an important source of resources for human populations  
204 (Moreno-Casasola, 2006). This factor has exerted direct pressure on the mangrove forest  
205 through deforestation for timber and fuel wood extraction, and more recently in the  
206 interruption of surface and subsurface flows in the by infrastructure of the oil industry.  
207 These local factors have been especially harsh on the northern sub-basin, where only sparse  
208 remnants of the mangrove forest survive today. Thus, whereas vigorous mangrove forests  
209 surround the southern sub-basin, the northern sub-basin is occupied by highly disturbed  
210 vegetation including sparse mangrove remnants. Regionally, growing human population  
211 and the parallel development of infrastructure apply further pressures to coastal ecosystems  
212 through pollution, accelerated erosion, increasing sea level, among other elements (Gilman  
213 et al., 2008).

214

### 215 **3. Methods**

#### 216 *3.1 Field work and laboratory analysis*

217 In autumn 2015, a 13-meter-long core was recovered from the southern part of La Mancha  
218 coastal lagoon (core MAN15V, Fig. 1), under an *A. germinans* stand, using a modified  
219 Livingston piston corer (Colinvaux et al., 1999). The core was longitudinally sectioned,  
220 stratigraphically described, and stored at ~ 4°C to preserve the sedimentary evidence. The  
221 chronological control of the sedimentary sequence was based on eight accelerator-mass-  
222 spectrometer (AMS) radiocarbon dates of bulk sediment, homogenously distributed along  
223 the core given that no other material such as macrofossils or charcoal could be found.  
224 Radiocarbon dates were calibrated to years before present (hereafter cal BP) using the

Formatted: Font: Italic

225 IntCal13 curve (Reimer et al., 2013), and calibrated dates were used to build a Bayesian  
226 age-depth model using Bacon (Blaauw and Christen, 2011). The core was subsampled  
227 every ~ 12.5 cm for pollen analysis, aiming at a temporal resolution of ~75 years between  
228 contiguous samples. A total of 104 samples were processed for pollen analysis using  
229 standard pollen extraction techniques (Faegri and Iversen, 1989). Samples were analyzed  
230 | under transmitted-light microscope [at magnifications of x400 and x1000](#), aiming to [reach](#) a  
231 minimum pollen sum of 300 pollen grains. Grains of the family Cyperaceae and  
232 pteridophytes spores were excluded from the pollen sum, although they were counted and  
233 included in the interpretation. Pollen counts were transformed into percentages of the  
234 pollen sum and a stratigraphic pollen diagram was constructed.

235 Pollen taxa were classified into five groups according to their modern ecological  
236 affinities (ecological affinities after Lugo and Snedaker 1974, Ranwell 1972, Travieso-  
237 Bello 2000): i) mangroves represented by *Rhizophora mangle*, *Avicennia germinans*, and  
238 *Conocarpus erectus*; although *Laguncularia racemosa* is an important component of the  
239 local mangrove forests, it was not found in the pollen spectra; ii) salt marsh vegetation  
240 represented by Cyperaceae, Amaranthaceae, *Croton*, *Typha*, Asteraceae, Chenopodiaceae,  
241 | and *Mimosa*; iii) lowland forest represented by *Inga*, *Acacia*, *Machaerium*, *Protium*,  
242 *Bursera*, and Moraceae-Urticaceae; iv) montane regional forests represented by *Alnus*,  
243 *Myrica*, Ulmaceae, *Quercus*, and *Miconia*; and v) disturbance taxa represented by *Pinus*  
244 and Poaceae; these latter taxa were classified as representatives of disturbance because in  
245 Mexico they are distributed along environments unfavorable to vegetation development,  
246 usually associated with either natural or anthropogenic causes (Franco-Gaviria et al., 2018;  
247 | Rzedowski, 2006). High abundances of *Pinus* pollen have been reported for areas [submitted](#)

248 | [subjected](#) to dry conditions and/or regimes of high disturbance (Correa-Metrio et al., 2013;  
249 | Metcalfe et al., 2000), mostly associated with early succession colonizers (Ramirez-Marcial  
250 | et al., 2001). Meanwhile, although Poaceae pollen is characteristic of successional  
251 | processes of supratidal plains (Bush, 2002; Urrego et al., 2013), it is also found in pollen  
252 | assemblages from all Mexican vegetation types, usually associated with disturbance  
253 | (Correa-Metrio et al., 2013; Franco-Gaviria et al., 2018).

254 |         The fossil pollen record was complemented by sampling 30 locations  
255 | homogeneously for modern mud-water interface (15 samples from each sub-basin)  
256 | distributed [along across](#) the water body, using an Ekman dredge. This sampling was meant  
257 | to cover the variability of the modern pollen spectra (Fig.1), especially the differences  
258 | between depositional environments of the two sub-basins. Samples were treated and  
259 | analyzed using the same techniques as the fossil samples.

260 |         Total both C (%TC) and N (%TN) were measured in fossil samples every 5 cm  
261 | along the core and in modern samples. For this purpose, samples were freeze dried and  
262 | crushed, and subsequently analyzed using a Carlo Erba NA1500 CNS elemental analyzer.  
263 | Additionally, coulometric titration was used to determine carbonate carbon (%TIC) in  
264 | modern samples, allowing the estimation of organic carbon (%TOC). The discrimination of  
265 | TC into TIC and TOC in modern samples was used to infer the relationship between these  
266 | two carbon sources in the system of La Mancha lagoon.

267 |

268 | *3.2 Statistical Analysis*

269 A non-metric multidimensional scaling ordination (NMDS) was applied on pollen relative  
270 abundances, including both modern and fossil samples. The ordination was performed to  
271 summarize the temporal variability of [the](#) pollen spectra, and to evaluate vegetation  
272 temporal dynamics in the context of the modern lagoon. This technique ordines samples  
273 on a  $k$ -dimensional space defined *a priori* by the analyst, aiming to maintain the original  
274 topologic relationships among samples (Legendre and Legendre, [19982012](#)). Although  
275 two-dimensional ordinations are readily used, we selected three dimensions to produce a  
276 relaxed ordination where the affinity among pollen spectra can manifest more freely. We  
277 used the Bray-Curtis metric to estimate dissimilarity among samples, a metric that relies  
278 more on compositional data than [in-on](#) the abundance of individual taxa and has been  
279 proven monotonic to ecological distance (Faith et al., 1987).

280 Modern samples were classified into southern and northern sub-basins as  
281 representative of dense and sparse mangrove forests, respectively. Whereas the northern  
282 sub-basin has direct contact with the sea through the ephemeral mouth, which creates a  
283 more energetic environment, and has been ~~submitted~~ [subjected](#) to important human  
284 disturbances and modifications resulting in sparse mangrove cover, the southern sub-basin  
285 is more influenced by the entrance of the river and is occupied by a well-developed dense  
286 mangrove stand. Thus, pollen spectra from these two sub-basins should reflect contrasting  
287 mangrove-forest cover conditions, and their relative oceanic and fluvial influences. The  
288 statistical significance of the difference between NMDS sample scores of the two sub-  
289 basins were tested using a two-sample t-test (Zar, 1999). [TIC, TOC, TC, and TN content in](#)  
290 [modern samples were compared using Pearson correlation coefficient, whereas](#)  
291 [comparisons of concentrations between the northern and southern sub-basins were also](#)  
292 [compared using two-sample t-test \(Zar, 1999\).](#)

293

## 294 4. Results

### 295 4.1 Stratigraphy and chronology of the sedimentary record

296 Sediments from [the](#) La Mancha coastal lagoon were mostly brownish, shelly clays with low  
297 content of organic material, and some intermissions of brownish silt with shell fragments  
298 and organic material (Fig. 2A). From the base of the core up to 1200 cm below lagoon floor  
299 (blf hereafter), the sediments were brown [shellish-shelly](#) clay, while from 1200 to 663 cm  
300 blf the color turned into a light brown matrix (clay and silt) with shell fragments and  
301 carbonates. From 663 to 615 cm blf the [clayish-clayey](#) sediments ~~were~~ brown with light  
302 brown bands. From 615 to 372 cm blf, the sediment showed brownish tones, and were  
303 mostly composed of clay with a thin layer of silt, [shellish-shelly](#) and little organic material.  
304 The uppermost 327 cm were dark to very light brown, with a uniform [shellish-shelly](#) clay  
305 composition (Fig 2A).

306 All radiocarbon dates resulted in stratigraphic order (Table 1). [Although bulk](#)  
307 [sediment dates could lead to an <sup>14</sup>C age offset, we were not able to quantify it because of](#)  
308 [the lack of other quantifiable materials. Nevertheless, the high correspondence between TC](#)  
309 [and TN along the sedimentary record \(Fig. 2\) suggests that inorganic carbon represents a](#)  
310 [relatively low proportion of the sedimentary material.](#) According to the age-depth model,  
311 the core has a basal age of ~7840 cal BP, resulting in an average sedimentation rate of 1.96  
312 mm/yr (Fig 2B). From the bottom of the sequence up to 5500 cal BP, sedimentation rates  
313 were high, with maximum values around 5500 cal BP (4.10 mm/yr). From c. 5500 cal BP  
314 to present, sedimentation rates showed a decreasing trend, reaching 0.89 mm/yr in the  
315 uppermost part of the core (Fig 2).

Formatted: Superscript

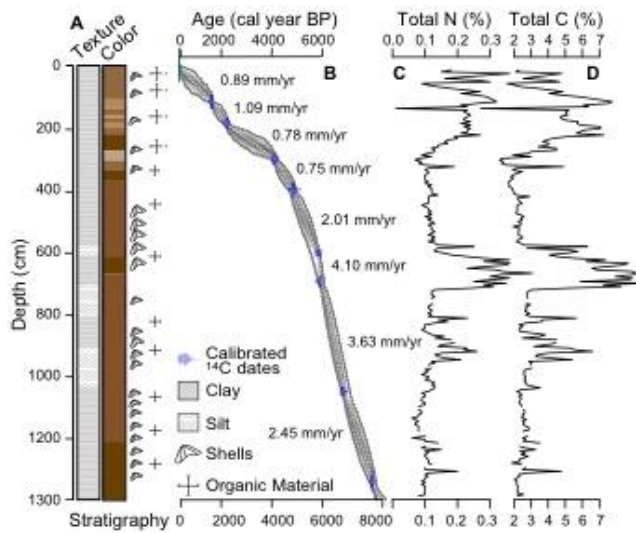
316

317 Table 1. Radiocarbon dates of core MAN15V from La Mancha coastal lagoon. Depths in

318 cm below lagoon floor (blf). [Ages calibrated after the IntCal13 curve \(Reimer et al., 2013\).](#)

Laboratory code	Depth (cm blf)	<sup>14</sup> C Age	Error	<u>Calibrated age</u> <u>(95% range; cal BP)</u>
UBA-34340	109	1290	24	<u>1181-1283</u>
Beta-440367	175	1880	30	<u>1730-1883</u>
UBA-34341	282	3447	26	<u>3637-3826</u>
Beta-440368	373	3970	30	<u>4300-4523</u>
UBA-34342	564	4732	41	<u>5326-5584</u>
Beta-437078	649	4770	30	<u>5334-5588</u>
UBA-34343	979	5624	41	<u>6312-6482</u>
Beta-437079	1249	6700	30	<u>7508-7616</u>

319



320

321

322 | Figure 2. Core MAN15V from La Mancha coastal lagoon. A. Stratigraphy of the  
323 | sedimentary sequence; texture (left) ~~and~~, color (right), and organic and shell content. B.  
324 | Age-depth model; calibrated ages (blue silhouettes), 95% confidence intervals in grey  
325 | (darker colors indicate higher probability), and sedimentation rates (mm/yr). C and D.  
326 | Percentage of total nitrogen and total carbon content (TN and TC, respectively).  
327 |  
328 |

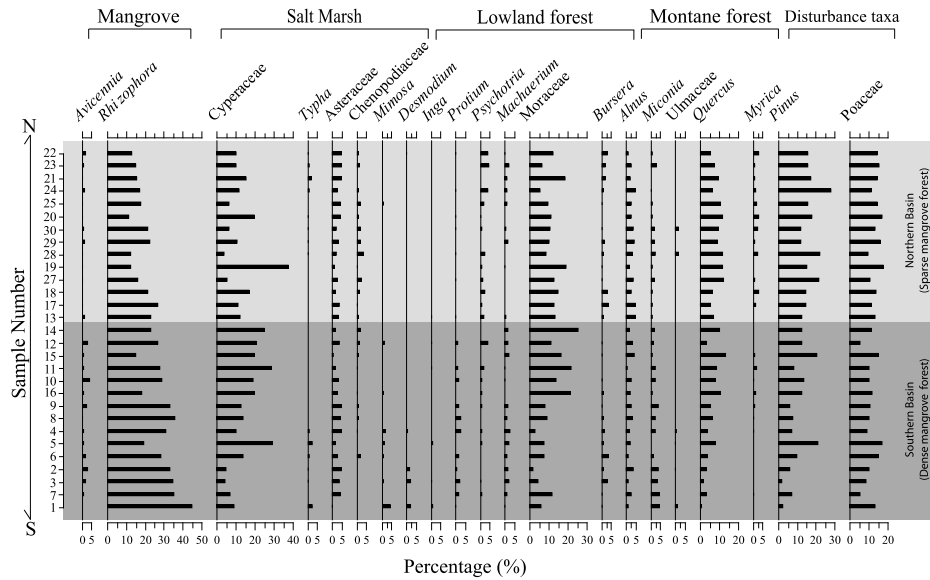
#### 329 | 4.2 ~~Modern p~~Pollen spectra and C and N in modern samples

330 | Modern samples were characterized by 49 taxa, 18 and 31 identified at family and genus  
331 | levels, respectively. Pollen sums varied between 300 and 387, whereas pollen counts  
332 | including Cyperaceae and pterodophytes were between 322 and 472 palynomorphs.  
333 | *Rhizophora*, Cyperaceae, Moraceae-Urticaceae, *Quercus*, *Pinus*, and Poaceae dominated  
334 | these samples (up to 45%), whereas taxa such as *Typha*, *Mimosa*, *Desmodium*, *Inga*, and  
335 | Ulmaceae were poorly represented (less than 5%). One sample from the northern sub-basin  
336 | ~~resulted was~~ barren of pollen (sample 26, Fig. 1).

337 | *Avicennia* and *Rhizophora* showed high percentages (up to 5 and 45%, respectively)  
338 | towards the southern sub-basin of the lagoon (Figs. 1 and 3). Contrastingly, other taxa such  
339 | as *Quercus*, *Myrica*, and *Pinus* decreased southwards. Compositional differences between  
340 | the northern and southern sub-basins of the lagoon were also ~~evidenced~~ indicated by taxa  
341 | that occurred only at the latter, such as *Desmodium*, *Inga*, and *Protium* (Figs. 1 and 3).

342 | Samples from the middle area of the lagoon (samples 12,13,14,17 and 18) (Figs. 1 and 3)  
343 | contained the highest percentages of Cyperaceae and Moraceae-Urticaceae (25% and 30%,  
344 | respectively), and minima of *Typha*, Asteraceae, and *Psychotria*. In the northern sub-basin

345 (Figs. 1 and 3), *Quercus*, *Pinus*, and *Poaceae* dominated the pollen spectra with abundances  
 346 above 10%.  
 347

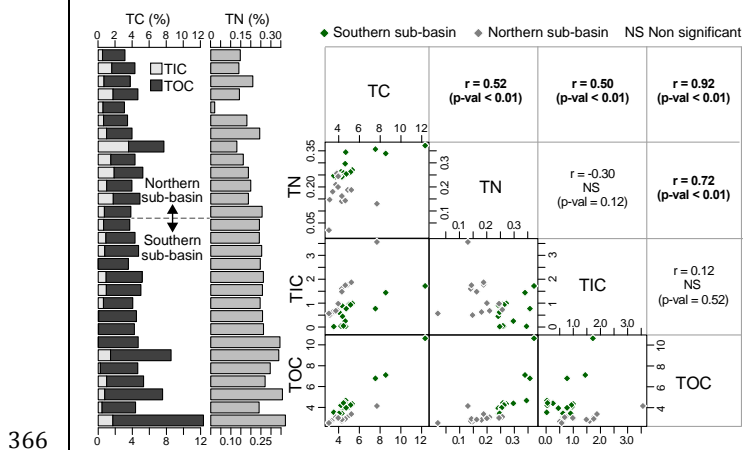


348  
 349 Figure 3. Pollen diagram of selected taxa from mud-water interface samples from La  
 350 Mancha coastal lagoon. Ecological affinities after Lugo and Snedaker (1974), Ramwell  
 351 (1972), [and](#) Travieso-Bello (2000). Samples are ordered from South to North with samples  
 352 from the southern (northern) sub-basin highlighted in dark (light) grey.

353  
 354 [TC content in modern samples varied between 3.1 and 12.3%, with mean and median of 4.9](#)  
 355 [and 4.4%, respectively. Although mean values for the northern and southern sub-basins](#)  
 356 [were not statistically differentiable \( \$t = 1.66\$ ,  \$p\text{-value} = 0.11\$ \), the northern sub-basin](#)  
 357 [consistently showed lower values \(Fig. 3\). Differently, individual fractions of C resulted](#)



358 statistically differentiable, with a higher concentration of TOC in the southern sub-basin  
 359 (3.56, p-value = 0.002) and a higher concentration of TIC in the northern sub-basin (t = -  
 360 2.47, p-value = 0.023). TN range between 0.02 and 0.37% with mean and median of 0.23  
 361 and 0.24%, respectively (Fig. 3), with higher mean concentration in the southern subbasin  
 362 (t = 5.54, p-value < 0.001). TC resulted statistically associated with TN, TIC, and TOC,  
 363 although the magnitude of the correlation was substantially higher with the latter (Fig. 3).  
 364 Whereas TIC resulted moderately associated only with TN, TOC was strongly associated  
 365 with both TC and TN (Fig. 3).



366  
 367 Figure 4. Content (%) of carbon and nitrogen in the modern samples of La Mancha coastal  
 368 lagoon. Total C content (TC) discriminated into inorganic and organic fractions (TIC and  
 369 TOC), and total N content (TN). Comparisons among sedimentary attributes are shown in  
 370 the right side panels (biplots and correlation coefficients with their significance).

371

372

373 | 4.3 ~~Fossil pollen~~Fossil record

374 Fossil pollen types included 55 taxa classified into 24 families and 31 genera. Pollen sums  
375 varied between 300 and 349 grains per sample (average 306 grains), whereas pollen counts  
376 that included Cyperaceae and pterodophytes reached between 303 and 359 palynomorphs  
377 per sample (average 317). The highest abundances were shown by *Rhizophora*, Moraceae-  
378 Urticaceae, *Quercus* and *Pinus*, while the lowest abundances were shown by *Conocarpus*,  
379 *Inga*, *Bursera* and *Miconia*. From within the 55 identified taxa, only *Rhizophora*,  
380 Cyperaceae, *Typha*, Asteraceae, Chenopodiaceae, Moraceae-Urticaceae, *Alnus*, *Quercus*,  
381 *Pinus*, and Poaceae persisted throughout the entire record. The record was discretized into  
382 four main pollen zones (Fig. 4) to facilitate the description of the sedimentary sequence.  
383 Pollen zones were defined based on an inspection of the distribution of pollen percentages  
384 though time, aiming to identify time periods characterized by relatively stable pollen  
385 assemblages.

386

387 | **Pollen Zone I (from 1300 to 907 cm blf, c. 7840-6300 cal BP):** The sediment showed TC  
388 concentrations between 1.84 and 4.78%, with mean of 2.54%, and TN concentrations  
389 between 0.06 and 0.20%, with mean 0.10% (Fig. 2). This zone showed high percentages of  
390 *Rhizophora* (up to 20%), Moraceae-Urticaceae (up to 50%), *Quercus* (up to 20%), *Pinus*  
391 (up to 50%), and Poaceae (up to 20%). Low percentages (less than 5%) were shown by  
392 *Avicennia*, Amaranthaceae, *Croton*, *Typha*, Asteraceae, Chenopodiaceae, *Mimosa*, *Inga*,  
393 *Acacia*, *Machaerium*, *Protium*, *Bursera*, Ulmaceae and *Miconia* (Fig.4).

394

395 **Pollen Zone II (from 907 to 569 cm blf, c. 6300 - 5400 cal BP):** The sediment showed  
396 highly variable concentrations of both TC and TN (Fig. 2). TC varied between 2.28 and  
397 9.67% with mean of 4.6%, whereas TN varied between 0.09 and 0.43 with a mean of  
398 0.19%. This zone was dominated by Cyperaceae (20%), *Croton* (10%), *Typha* (20%),  
399 Chenopodiaceae (15%), Moraceae-Urticaceae (50%), *Alnus* (~6%), Ulmaceae (10%),  
400 *Quercus* (20%), *Pinus* (50%) and Poaceae (20%). Percentages below 5% were shown by  
401 *Avicennia*, *Conocarpus*, Amaranthaceae, Asteraceae, *Mimosa*, *Inga*, *Machaerium*, *Protium*,  
402 *Bursera* and *Miconia* with less than 5%. The upper part of the zone was characterized by  
403 relatively low percentages of *Pinus* (~18%) and a substantial increase of Amaranthaceae,  
404 *Croton*, *Typha*, Asteraceae, Chenopodiaceae, and Cyperaceae (up to ~20%) (Fig. 4).

405

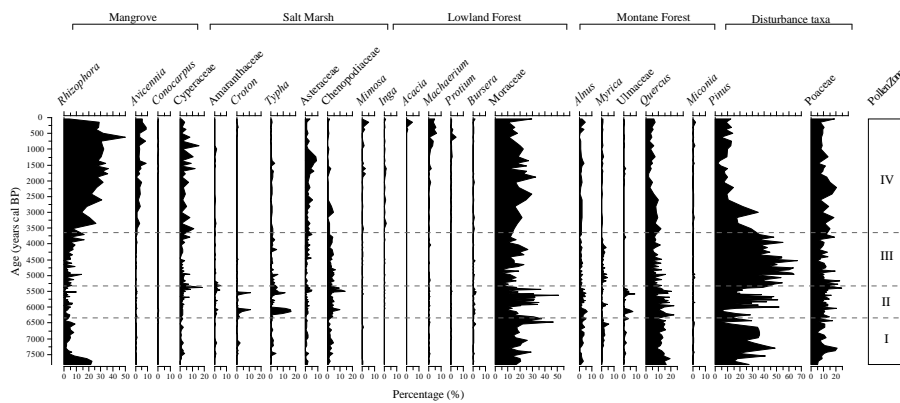
406 **Pollen Zone III (from 569 to 280 cm blf, c. 5400 - 3700 cal BP):** With lower variability,  
407 both TC and TN decreased substantially (Fig. 2). TC varied from 1.14 and 6.31% with  
408 mean of 2.45, and TN varied between 0.07 and 0.25% with mean of 0.12%. From 5400 BP  
409 *Rhizophora* abundances began to increase gradually, and *Avicennia* ~~showed was~~ less than  
410 5%. *Pinus* reached the highest abundances throughout the record (up to 60%), while  
411 Amaranthaceae, *Croton*, *Mimosa*, *Inga*, *Machaerium*, *Bursera*, *Alnus*, Ulmaceae,  
412 Moraceae-Urticaceae, and *Miconia* showed their lowest percentages. Lastly, *Typha*,  
413 Asteraceae, and Chenopodiaceae showed abundances around 10% (Fig 4).

414

415 **Pollen Zone IV (from 280 to 0 cm blf, c. 3700 cal BP - Present):** TC and TN  
416 progressively reached high variable concentrations (Fig. 2). TC varied between 0.02 and  
417 7.77% with mean of 4.45%, and TN varied between 0.01 and 0.36% with mean of 0.20%.  
418 Abundances of *Rhizophora* and *Avicennia* reached their highest values (up to 60% and 10%

419 respectively), and displayed an increasing trend towards the present. Amaranthaceae,  
 420 *Croton*, *Typha*, Chenopodiaceae, *Myrica*, Ulmaceae, *Quercus*, and *Pinus* abundances  
 421 decrease up to the present. Meanwhile *Acacia*, *Inga*, *Machaerium*, and *Protium* presented  
 422 their highest abundances (up to 10%) (Fig. 4).

423



424

425 Figure 45. Fossil pollen diagram of selected taxa of core MAN15V from La Mancha  
 426 coastal lagoon. (ecological affinities after Lugo and Snedaker 1974, Ramwell 1972, and  
 427 Travieso-Bello 2000, and Castillo-Campos 2006).

428

#### 429 4.4 Statistical analyses

430 The three-dimensional ordination of the modern and fossil pollen samples showed a stress  
 431 of 0.144. Negative scores along Axis 1 characterized modern samples, whereas fossil  
 432 samples were clearly divided into positive (negative) scores for samples older (younger)  
 433 than ~ 5400 cal BP (Fig. 5 and 6.B). Along Axis 2, both modern and fossil samples were  
 434 mostly located between -0.31 and 0.2, although fossil samples showed positive and

435 negative excursions (Fig. 5). NMDS Axis 3 was characterized by widespread scores for  
436 fossil samples and almost exclusively negative [scores](#) for modern samples (Appendix 1).

437 The t-test for comparing NMDS scores of modern samples from the northern and  
438 southern sub-basins yielded significant differences in terms of Axis 1 and 2, but non-  
439 significant for Axis 3 (Table 2). Given the relatively flat behavior of Axis 2 and the lack of  
440 significance of Axis 3 (Appendix 1), only the first axis of the ordination will be considered  
441 for interpretations hereafter.

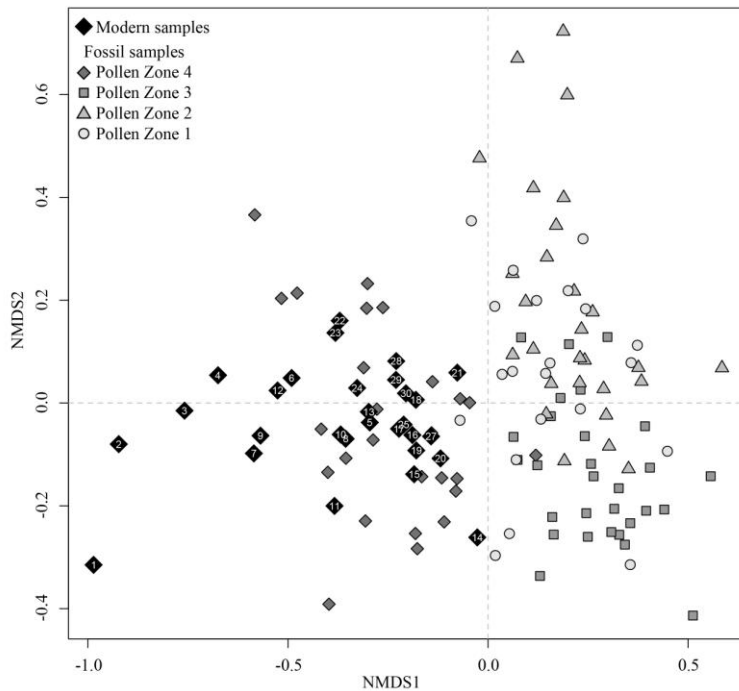
442

443 Table 2. Comparison of NMDS sample scores in the three axes for modern samples from  
444 the northern and southern sub-basins, i.e scores from dense (D) vs. sparse (S) mangrove  
445 areas. For the comparison of scores along each axis, t scores, degrees of freedom corrected  
446 for variance differences between samples (d.f.), and p-value are shown.

447

Comparison	t	d.f.	p-value
Axis 1 <sub>D</sub> – Axis 1 <sub>S</sub>	-3.5184	18	0.0026
Axis 2 <sub>D</sub> – Axis 2 <sub>S</sub>	-2.7661	26	0.0103
Axis 3 <sub>D</sub> – Axis 3 <sub>S</sub>	1.3831	24	0.1796

448



449

450 | Figure 56. Non-metric multidimensional scaling for modern and fossil pollen assemblages  
 451 | from La Mancha lagoon. Modern samples in black diamonds showing sample number,  
 452 | whereas fossil samples were symbol coded according to the declared legend.

453

454 | **5. Discussion**

455 | 5.1 Modern pollen spectra sediments of La Mancha coastal lagoon

456 | Palynological composition of modern samples generally reflected the patterns of modern  
 457 | vegetation, incorporating vegetation elements from the surrounding mangroves and salt  
 458 | marshes (local vegetation), and nearby lowlands and highland forest (regional vegetation).  
 459 | Although the mangroves of La Mancha are dominated by *A. germinans* over *R. mangle*  
 460 | (Moreno-Casasola, 2006), modern pollen spectra were dominated by the latter (Fig. 3).

461 Given its pollination mechanism, *R. mangle* produces high amounts of pollen, dominating  
462 most of pollen spectra from mangrove forests. Contrastingly, *A. germinans* is an insect-  
463 pollinated species that produces low amounts of pollen (Hogarth, 2007), resulting in under-  
464 representation of the parental taxon in the pollen spectra where percentages as low as 5%  
465 implying an important share in the standing vegetation. However, the mean representation  
466 of *R. mangle* in modern samples from the densely mangrove-forested [southern](#) sub-basin  
467 (~25%) are low as compared to pollen spectra from stands dominated by this species which  
468 have been reported as high as 65% (e.g. Behling et al., 2001; Urrego et al., 2009). Although  
469 *C. erecta* and *L. racemosa* are components of the standing forest of La Mancha, they are  
470 not represented in the modern pollen spectra probably because of their low production, and  
471 also because of their distal position with respect to the sampled water body (~~Fovilla and De~~  
472 ~~la Lanza, 1999~~[Moreno-Casasola, 2006](#)).

473 [At](#)~~In~~ the southern sub-basin of La Mancha, the high percentages of *Rhizophora*  
474 reflect the relatively [good](#) conservation ~~stage~~ of the mangroves (Moreno-Casasola, 2006),  
475 with the exclusive presence of taxa such as *Desmodium*, *Inga* and *Protium* indicating a well  
476 ~~preservation of~~[ed](#) lowland vegetation as well (Franco-Gaviria et al., 2018). Pollen spectra  
477 from the northern sub-basin contained lower percentages of *Rhizophora*, and a substantial  
478 representation of regional pollen, possibly coming from the highlands of the catchment  
479 basin. ~~Through the last~~[Over recent](#) decades, the deleterious effects of human activities on  
480 mangrove cover have been more intense around the northern sub-basin of La Mancha  
481 lagoon (Lopez-Portillo et al., 2011; Moreno-Casasola, 2006), reflecting on pollen  
482 assemblages where the regional and disturbance elements are better represented (mainly  
483 Moraceae-Urticaceae, *Myrica*, *Pinus*, Poaceae, and *Quercus*) (Correa-Metrio et al., 2011;

484 Franco-Gaviria et al., 2018). Although *Rhizophora*, Moraceae-Urticaceae, *Pinus*, and  
485 *Quercus* do not dominate the shore vegetation of the most disturbed northern areas, they are  
486 represented by pollen percentages above 10 % each (Fig. 3), reflecting the sparse nature of  
487 mangrove forests over this area. This finding reflects the widely reported  
488 overrepresentation of these taxa in pollen spectra, derived from their high production of  
489 pollen and their long-distance pollen dispersal capacity, as reported for species of  
490 anemophyllous pollination (e.g. Correa-Metrio et al., 2013; Ellison, 2008; Hooghiemstra et  
491 al., 2006; Marchant et al., 2002).

492 Modern samples ~~resulted were~~ clustered in the NMDS (Fig. 5), implying more  
493 consistency among ~~the~~ modern pollen spectra than between modern and fossil samples.  
494 This finding demonstrates that the modern heterogeneity of the lagoon does not represent  
495 the ecological and environmental variability of the area over the last ~7800 years.  
496 Statistically significant differences between the NMDS Axis 1 scores of pollen assemblages  
497 from the two sub-basins demonstrate that density of mangrove forest cover can be  
498 identified though their pollen spectra. Overall, these findings ~~imply indicate~~ that i) pollen  
499 assemblages of La Mancha lagoon are systematically associated with physical and  
500 biological attributes of the region at a broad scale (regional vegetation), and ii) pollen  
501 spectra are highly sensitive to the modern environmental variability ~~that express~~ throughout  
502 La Mancha lagoon (local vegetation). Thus, as reported for other areas (e.g. Franco-Gaviria  
503 et al., 2018; Urrego et al., 2009; Urrego et al., 2010), modern pollen assemblages of our  
504 studied lagoon provide a robust framework for interpreting our fossil pollen sequence.

505 Higher concentrations of TOC and TN in the southern sub-basin were probably a  
506 result of differences in surrounding vegetation and energy of the depositional environment.



507 More vigorous vegetation in the southern sub-basin would produce higher amounts of  
508 organic matter rich in TOC and TN, whereas the lower energy of the depositional  
509 environment would prevent resuspension and, therefore, further oxidation of the sediments  
510 (Meyers, 1997). Differently, TIC resulted higher in the northern sub-basin, probably  
511 reflecting both higher contribution of marine particulate suspended matter and more  
512 oxidation of organic components (Bouillon et al., 2003). Overall, C and N analyses are  
513 consistent with higher organic matter storage in the sediments of the lagoon where  
514 mangrove forests are well preserved. The relationships that were found between the  
515 different components of C and N demonstrate that in the modern setting of La Mancha,  
516 TOC is the main component of TC. Although these relationships cannot be extrapolated to  
517 the fossil record, they demonstrate that TN is a good proxy for organic matter, and  
518 therefore it is used to offer further support to our pollen-based reconstruction of past  
519 environmental dynamics.

520

## 521 *5.2 Vegetation history of La Mancha Lagoon*

522 The pollen record of La Mancha lagoon reflects the complexities associated with the  
523 multiple factors that have intervened in the development toward the modern biotic and  
524 abiotic systems. Whereas highly variable abundances of regional vegetation suggest  
525 variability in freshwater input by precipitation and tributaries to the lagoon system, pollen  
526 from mangroves together with herbaceous vegetation offer insights into the successional  
527 patterns and development of the local vegetation (Urrego et al., 2013; Urrego et al., 2018).  
528 Additionally, the constant presence of marine shells through the sedimentary record (Fig. 2)  
529 demonstrates a permanent marine influence through the last ~7,800 year. Together, these

530 indicators illustrate the intimate interaction between sea levels and regional fresh water  
531 inputs (precipitation, sediments) that ultimately regulates the colonization, establishment,  
532 and development of mangrove ecosystems in the area. According to our pollen [and](#)  
533 [geochemical](#) data, the history of the vegetation that surrounds the lagoon and therefore the  
534 regional environmental history could be summarized in four main stages that will be  
535 discussed below.

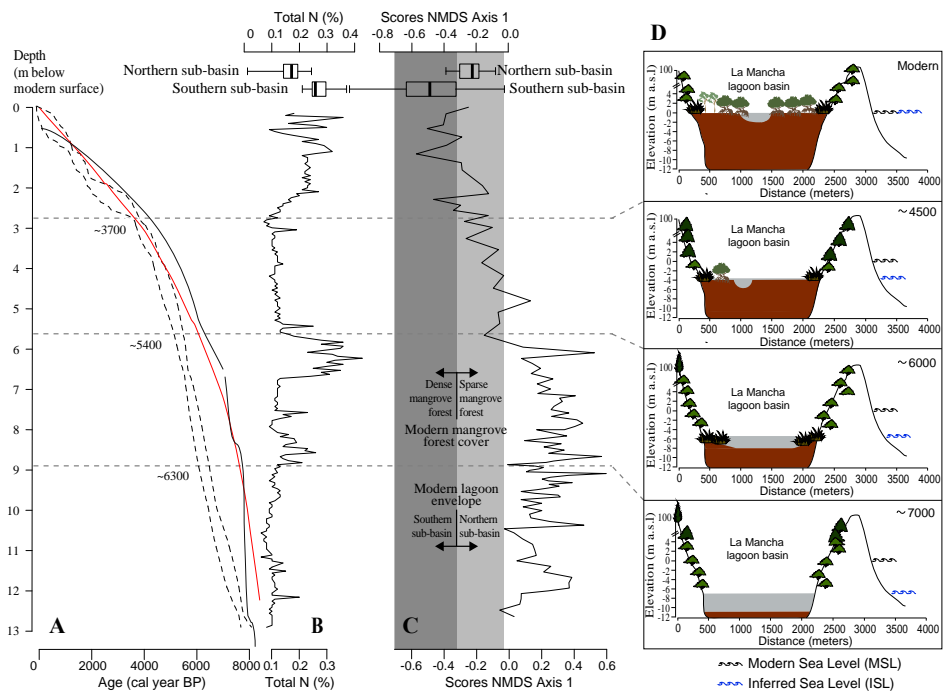
536 *From c.7800 to 6300 cal BP: sea-water flooding of valleys*

537 ~~Through this time period, the mud-water interface was between 13 and 9 m below the~~  
538 ~~modern surface, which today is at sea level. At the same time, average sea level was~~  
539 ~~between 9 and 5 m below modern. The difference between mud-water interface depth and~~  
540 ~~sea level can only be accounted by lagoon water depth, which~~ ~~The comparison of our age-~~  
541 ~~depth model with the reported increase of regional sea levels suggests that throughout this~~  
542 ~~time period the mud-water interface~~ was around ~~6~~~ 4 m below sea level (Fig. 6A). La  
543 Mancha Hill, an andesitic rock of Neogene origin (~~García-Gil~~ [Moreno-Casasola](#), 2006;  
544 Geissert [Kientz](#), 1999) (Fig. 1), probably acted as a barrier that protected the depositional  
545 environment from the erosive energy of the waves and winds. Through this period, even  
546 though sedimentation rates at La Mancha (~3.04 mm/year) were lower than the inferred  
547 rate of sea-level increase, they are among the highest through the record. High rates of both  
548 regional sea-level rise and sedimentation at La Mancha are likely a result of the regional  
549 geologic instability that characterized the conformation ~~processes~~ of the modern Gulf of  
550 Mexico in its final stages, up to 5000 cal BP (Davis, 2011; [Pirazzoli, 1990](#)). As sea level  
551 increased through the deglaciation and the early Holocene, sea-water flooded coastal plains  
552 and valleys at a speed that surpassed the accumulation of continental sediments. Thus, the

553 lacustrine basin of La Mancha was probably deeper ~~than modern and bucket-shaped~~,  
554 impeding the establishment of mangrove forests (Fig. 6C). A peak of *Rhizophora* from the  
555 bottom of the record to ~7500 cal BP (Fig. 4) probably shows the colonization of  
556 mangroves during the initial stages of the lagoon and the sea-water flooding, which were  
557 subsequently displaced by the formation of a deep-water body.

558 In México, *Pinus* populations thrive under early post-disturbance successional  
559 stages, or under conditions that are not optimal for other taxa (Metcalfé et al., 2000;  
560 Ramírez-Marcial et al., 2001). Thus, the persistence of *Pinus* in high percentages from the  
561 bottom of the record to ~6500 cal BP (Fig. 5) indicates that regional conditions were likely  
562 dry, an interpretation that is further supported by the lowest concentrations of TN (Fig. 7)  
563 and therefore of organic matter. These dry conditions probably played a central role at  
564 maintaining sedimentation rates that did not offset sea-level rise, impeding the  
565 establishment of mangrove forests, as demonstrated by the NMDS Axis 1 scores that were  
566 outside the envelope defined by modern samples (Fig. ~~6B~~7C).

567



Formatted: Font: (Default) Times New Roman, 12 pt

568  
 569 Figure 67. Environmental history of La Mancha Lagoon through the last 7,800 years. A.  
 570 Age-depth model of core MAN15V from La Mancha Lagoon (dashed lines show 95%  
 571 confidence interval), compared with sea level rise curves for the Caribbean (red line,  
 572 Toscano and Macintyre, 2003) and the northern Gulf of Mexico (black solid line, Milliken  
 573 and Anderson, 2008). B. [Sedimentary total nitrogen content \(%\)](#); [boxplots illustrate total](#)  
 574 [nitrogen in modern samples form the northern \(up\) and southern \(down\) sub-basins of the](#)  
 575 [lagoon \(whiskers show minimum and maximum scores\)](#). C. NMDS Axis 1 scores through  
 576 time; boxplots illustrate scores of modern samples [form the northern \(up\) and southern](#)  
 577 [\(down\) sub-basins of the lagoon \(whiskers show minimum and maximum scores\)](#); scores of  
 578 the modern environmental envelope represented by modern samples are highlighted in  
 579 grey; scores of the interquartile range of samples from the well preserved southern sub-

Formatted: Font: Bold

580 basin are in dark grey. [CD](#). Schematic development of La Mancha Lagoon, illustrated at  
581 ~7,000, 6000, 4,500 cal BP, and Modern.

582

583

584 *From c. 6300 to 5400 cal BP: development of lagoon shores*

585 Whereas the rate of sea-level rise started to decline through this period, sedimentation rates  
586 at La Mancha remained high (3.86 mm/yr, Fig. 6). This phenomenon could be explained by  
587 two critical factors: i) following the reported deceleration of sea-level rise at ~7000 cal BP  
588 (Toscano and Macintyre, 2003), sand bars started accumulating at the mouth of coastal  
589 lagoons (Davis, 2011), providing a more stable plain for sediment accumulation at La  
590 Mancha; and ii) a substantial decrease in the percentages of *Pinus*, and an increase of  
591 montane forest taxa (e.g. *Alnus*, *Quercus*, and *Ulmaceae*) indicate wetter conditions that  
592 would be in turn associated with higher river sediment discharge. These regional wetter  
593 conditions could be related to the final stages of the Holocene Thermal Maximum, which  
594 was in general characterized by higher than present precipitation and temperature in the  
595 Northern Hemisphere (Renssen et al., 2009).

596 The lagoon became shallower, and the development of muddy shores is evidenced  
597 by high percentages of salt marsh vegetation ([Fig. 5](#)), and high accumulation of organic  
598 matter revealed by the increasing TN ([Fig. 7B](#)). This state of local vegetation and the high  
599 accumulation of organic matter suggest ~~a process also favored by the slowing rates of sea~~  
600 ~~level rise (Fig. 6A), with dominance of pollen spectra by salt marsh taxa indicating also~~  
601 ~~more tidal influence (González et al., 2010; Ranwell, 1972).~~ The closing of the ephemeral

602 | mouth, ~~was~~ probably caused by lower energy associated with the shallowing of the lagoon,  
603 | together with the intensification of the wind currents, and sea level changes reported for the  
604 | Gulf of Mexico and the Caribbean (Balsille and Donoghue, 2004; González and Dupont,  
605 | 2009; Urrego et al., 2013; Wooller et al., 2007). Pollen spectra suggest the early stages of a  
606 | successional pattern of mangrove vegetation associated with the marine transgression,  
607 | although NMDS Axis 1 sample scores demonstrate that mangrove forests were not  
608 | established yet near the location where the core was retrieved.

609 | *From c. 5400 to 3700 BP: A regional drought*

610 | Whereas the rate of sea-level rise continued to decrease, relatively high sedimentation rates  
611 | were evident in La Mancha sequence up to ~5000 cal BP, when apparently the rates  
612 | ~~deposition~~ of sediments deposition in the lagoon and those of sea level rise became similar  
613 | (Fig. 6A). Such equilibrium between sediment deposition and sea-level rise implies the  
614 | definition of a coastal erosive baseline that ~allowed the deposition of sand in the coast by  
615 | the northerly currents during the dry season, creating the sandbar that dams the lagoon.  
616 | Differently, during the wet season, the fluvial input would have the capacity to erode the  
617 | sandbar, opening the direct contact between the lagoon and the sea and, thus, resulting in  
618 | the modern seasonal flood cycle ~~of the lagoon~~. During the dry season, the coastal bar would  
619 | be closed by the action of the waves and the prevailing winds, whereas during the rainy  
620 | season the bar would be opened by the energy of the fresh water discharge. The lagoon thus  
621 | became a shallow water body ( $z_{\max} \sim 1$  m) mostly protected from the energy of the waves by  
622 | La Mancha hill (Fig.1), and subjected to seasonal tidal and climatic fluctuations.

623 | From c. 5400 to 3700 cal BP, the recurrent drainage of fresh water into the sea  
624 | probably created a series of canals-channels giving the lagoon a physiography very similar

625 to modern. However, according to the NMDS scores, vegetation at that time resembled the  
626 northern sub-basin today (Fig. 6B), an area characterized by poorly developed sparse  
627 mangrove stands. Thus, vegetation assemblages from this period were a result of  
628 suboptimal environmental conditions for mangrove forest development. High percentages  
629 of *Pinus* (up to 60%) through this period suggest that there was a regional drought in place,  
630 which likely maintained high substrate salinity by reducing freshwater river discharge to  
631 the lagoon. Thus, local vegetation consisted of a mixture of sparse mangrove trees with  
632 some salt marshes species, and a slow increase of mangrove pollen because of the  
633 prevailing dry conditions (Fig. 4). Although anthropogenic influence cannot be discarded as  
634 a plausible explanation for the sparse mangrove vegetation, the inference of a regional  
635 drought is supported by similar reports from Lake Petén Itzá between ~ 4500 up to ~3000  
636 cal BP, Lake Tzib (Quintana Roo) at ~3500 cal BP (Carrillo-Bastos et al., 2010; Mueller et  
637 al., 2010), and also in the Cariaco Basin record, with a trend from ~5400 up to the present  
638 (Haug et al., 2001). Furthermore, the abrupt decrease of TN and its linear trend towards  
639 even lower concentrations (Fig. 7B) evidence rather oxidizing conditions, an environmental  
640 process that is difficult to explain from the perspective of human occupation.

641

642 *From c. 3700 cal BP to Present: the establishment of modern mangrove forests*

643 Mangrove pollen taxa showed the highest percentages (Fig. 5), ~~which reflected~~ indicating an  
644 environment of relative stability where the exchange of saline and fresh water, and the  
645 input of sediments were balanced, producing an increase of mangrove forest biomass  
646 (Krauss et al., 2008). These conditions provided consolidated clay sediments, where as  
647 indicated by the NMDS scores, mangrove forests developed into mature forest stands of  
648 *Rhizophora* and *Avicennia*. Increasing concentrations of TN (Fig. 7B) indicate high

649 | [accumulation of organic matter probably associated with the establishment of the mangrove](#)  
650 | [forest \(Bouillon et al. 2003\)](#). Sea level continued to increase at slower rates (Balsille and  
651 | Donoghue, 2004) that were matched by the rate of sediment accumulation in La Mancha  
652 | (~0.92 mm/yr on average). These more stable conditions for coastal ecosystems have been  
653 | reported for other localities in the Caribbean coinciding with other records (Urrego et al.,  
654 | 2013), where mangrove forests developed under a relatively stable sedimentation rate (1.09  
655 | to 0.89 mm/yr).

656 | *Pinus* and salt marsh pollen in La Mancha showed substantial decreases caused by  
657 | wetter conditions and higher representation of local mangrove pollen, implying a lower  
658 | regional influence on pollen spectra, and the continuation of the successional processes that  
659 | led to the establishment of the mangrove forest (González and Dupont, 2009). At this stage,  
660 | the lagoon seems to have reached its modern configuration, with influences from local  
661 | processes like the annual opening of the ephemeral mouth, fluctuating floods of salt water,  
662 | input of fresh water from the streams, and anthropogenic activities (Moreno-Casasola,  
663 | 2006). Indeed, the sharp decrease of *Rhizophora* is likely reflecting the terrestrialization of  
664 | the cored site, which today is occupied by an *Avicennia germinans* forest that floods only  
665 | when the ephemeral mouth is closed and the lagoon reaches its maximum water level  
666 | through the year. [This latter observation is further supported by the high variability of TN](#)  
667 | [concentrations towards the top of the record.](#)

668 |

## 669 | **6. Conclusion**

670 | The sedimentary record of La Mancha lagoon encompasses the history of ~~the~~ local and  
671 | regional environmental conditions through the last ~8,000 years, including the



672 establishment of modern mangrove forest along the coast of Veracruz. The record shows  
673 the regional context under which the coastal lagoon formed, showing the transformation of  
674 the lagoon from a water body with permanent communication with the sea to the modern  
675 seasonally closed system. When sea level rise rates were higher than the rates of sediment  
676 infill of the lagoon's basin, the depositional environment was under sea level and pollen  
677 assemblages were dominated by regional taxa. The ecological succession towards the  
678 establishment of mangrove forest started at ~6,300 cal BP, but mangrove forests were  
679 sparse, resembling those of the modern northern sub-basin because of two main reasons: i)  
680 the water column was relatively deep and sedimentary plains for mangrove establishment  
681 were likely narrow, and ii) a regional drought lasting from ~5400 to 3700 BP probably  
682 caused extremely high substrate salinity that impeded mangrove forests expansion. Dense  
683 mangrove forests alike those that occupy the southern sub-basin today established around  
684 ~3500 BP, and have dominated the area ever since.

685 The ~~pairing-matching~~ of lagoon sediment and sea levels at ~4000 cal BP was likely  
686 associated with the development of the seasonally open mouth. This pairing of lagoon  
687 sedimentary accumulation and sea levels defined the latter as the base level for erosion,  
688 allowing the accumulation of material during the dry season, and therefore the formation of  
689 a damming bar, which would eventually be ~~eventually~~ open during the rainy season owing  
690 to the increased freshwater discharge. Concomitant to this process would be the linear  
691 erosion of ~~canals~~ channels through the sedimentary deposit, conforming the modern  
692 geomorphology of the area. The establishment of the mangrove forest implied a substantial  
693 increase of sedimentary organic matter, highlighting the role of these ecosystems at storing  
694 carbon. Overall, our record demonstrates the complexity of the interactions between local

695 and regional factors in the development and evolution of both coastal geomorphology and  
696 ecosystems.

697

## 698 **Acknowledgements**

699

700 This research was funded by Programa de Apoyo a Proyectos de Investigación e  
701 Innovación Tecnológica PAPIIT-UNAM [grant number IN107716], and Consejo Nacional  
702 de Ciencia y Tecnología [grant number 256406]. [Alex Correa-Metrio was supported by](#)  
703 [Programa de Apoyos para la Superación del Personal Académico de la UNAM \(PASPA\).](#)  
704 Dayenari Caballero-Rodríguez, Esmeralda Cruz Silva, Roberto Maya Hernández, and  
705 Yosahandy Vázquez Molina are thanked for their assistance in the field.

706

## 707 **7. References**

- 708 Ball, M.C., 2002. Interactive effects of salinity and irradiance on growth: implications for mangrove  
709 forest structure along salinity gradients. *Trees*, 16, 126-139.
- 710 Balsillie, J.H., Donoghue, J.F., 2004. High resolution sea-level history for the Gulf of Mexico since  
711 the last glacial maximum. Florida Geological Survey.
- 712 Behling, H., Cohen, M.C.L., Lara, R.J., 2001. Studies on Holocene mangrove ecosystems dynamics  
713 of the Braganca Peninsula in north-eastern Para, Brazil. *Palaeogeography, Palaeoclimatology, Palaeoecology*, 167, 225-242.
- 714 Blaauw, M., Christen, J.A., 2011. Flexible paleoclimate age-depth models using an autoregressive  
715 gamma process. *Bayesian Analysis*, 6, 457-474.
- 716 Bouillon, S. et al., 2008. Mangrove production and carbon sinks: a revision of global budget  
717 estimates. *Global Biogeochemical Cycles*, 22.
- 718 Bouillon, S., Dahdouh-Guebas, F., Rao, A., Koedam, N., Dehairs, F., 2003. Sources of organic carbon  
719 in mangrove sediments: variability and possible ecological implications. *Hydrobiologia*,  
720 495, 33-39.
- 721 Bush, M.B., 2002. On the interpretation of fossil Poaceae pollen in the lowland humid neotropics.  
722 *Palaeogeography, Palaeoclimatology, Palaeoecology*, 177, 5-17.
- 723 Carrillo-Bastos, A., Islebe, G.A., Torrescano-Valle, N., González, N.E., 2010. Holocene vegetation  
724 and climate history of central Quintana Roo, Yucatan Peninsula, Mexico. *Review of*  
725 *Palaeobotany & Palynology*, 160, 189-196.
- 726 Colinvaux, P., de Olivera, P.E., Moreno, P.J.E., 1999. *Amazon Pollen Manual and Atlas*. Harwood  
727 Academic Publishers, Amsterdam.
- 728

Formatted: Spanish (Mexico)

Formatted: Spanish (Mexico)

- 729 Correa-Metrio, A., Bush, M.B., Lozano-García, M.S., Sosa-Nájera, S., 2013. Millennial-scale  
730 temperature change velocity in the continental northern Neotropics. *PLoS ONE*, 8, e81958.
- 731 Correa-Metrio, A., Bush, M.B., Pérez, L., Schwalb, A., Cabrera, K.R., 2011. Pollen distribution along  
732 climatic and biogeographic gradients in northern Central America. *The Holocene*, 21, 681-  
733 692.
- 734 Davis, R.A., 2011. Sea-level change in the Gulf of Mexico. Texas A&M University Press, Corpus  
735 Christi.
- 736 Ellison, J.C., 1989. Pollen analysis of mangrove sediments as a sea-level indicator: assessment from  
737 Tongatapu, Tonga. *Palaeogeography, Palaeoclimatology, Palaeoecology*, 74, 327-341.
- 738 Ellison, J.C., 2008. Long-term retrospection on mangrove development using sediment cores and  
739 pollen analysis: a review. *Aquatic Botany*, 89, 93-104.
- 740 Faegri, K., Iversen, J., 1989. Textbook of pollen analysis. 4th ed. Wiley, Chichester.
- 741 Faith, D.P., Minchin, P.R., Belbin, L., 1987. Compositional dissimilarity as a robust measure of  
742 ecological distance. *Vegetatio*, 69, 57-68.
- 743 FAO-UNEP, 2007. The world's mangroves 1980–2005. FAO Forestry Paper.
- 744 Feller, I.C., Friess, D.A., Krauss, K.W., Lewis, R.R., 2017. The state of the world's mangroves in the  
745 21st century under climate change. *Hydrobiologia*, 803, 1-12.
- 746 Franco-Gaviria, F. et al., 2018. The human impact imprint on the modern pollen spectra of the  
747 Maya lands. *Boletín de la Sociedad Geológica Mexicana*, 70, 61-78.
- 748 Geissert Kientz, D., 1999. Regionalización geomorfológica del estado de Veracruz. *Investigaciones  
749 geográficas*, 23-47.
- 750 Gilman, E.L., Ellison, J., Duke, N.C., Field, C., 2008. Threats to mangroves from climate change and  
751 adaptation options: a review. *Aquatic botany*, 89, 237-250.
- 752 González, C., Dupont, L.M., 2009. Tropical salt marsh succession as sea-level indicator during  
753 Heinrich events. *Quaternary Science Reviews*, 28, 939-946.
- 754 González, C., Urrego, L.E., Martínez, J.I., Polanía, J., Yokoyama, Y., 2010. Mangrove dynamics in the  
755 southwestern Caribbean since the 'Little Ice Age': A history of human and natural  
756 disturbances. *The Holocene*, 20, 849-861.
- 757 Hamilton, S.E., Casey, D., 2016. Creation of a high spatio-temporal resolution global database of  
758 continuous mangrove forest cover for the 21st century (CGMFC-21). *Global Ecology and  
759 Biogeography*, 25, 729-738.
- 760 Haug, G.H., Hughen, K.A., Sigman, D.M., Peterson, L.C., Rohl, U., 2001. Southward migration of the  
761 Intertropical Convergence Zone through the Holocene. *Science*, 293, 1304-1308.
- 762 Hogarth, P.J., 2015. The biology of mangroves and seagrasses. Oxford University Press, Oxford.
- 763 Hooghiemstra, H., Lézine, A.M., Leroy, S.A.G., Dupont, L., Marret, F., 2006. Late Quaternary  
764 palynology in marine sediments: A synthesis of the understanding of pollen distribution  
765 patterns in the NW African setting. *Quaternary International*, 148, 29-44.
- 766 Kjerfve, B., 1994. Coastal lagoon processes. Elsevier, Amsterdam.
- 767 Krauss, K.W. et al., 2008. Environmental drivers in mangrove establishment and early  
768 development: a review. *Aquatic Botany*, 89, 105-127.
- 769 Lankford, R.R., 1977. Coastal lagoons of Mexico their origin and classification, *Estuarine Processes:  
770 Circulation, Sediments, and Transfer of Material in the Estuary*. Elsevier, pp. 182-215.
- 771 Legendre, P., Legendre, L., 2012. Numerical Ecology. Elsevier Scientific, Oxford.
- 772 López-Portillo, J., 2011. Atlas de las costas de Veracruz: manglares y dunas [costeras]. Gobierno del  
773 Estado de Veracruz, Secretaría de Educación, Xalapa.
- 774 Lugo, A.E., Snedaker, S.C., 1974. The ecology of mangroves. *Annual review of ecology and  
775 systematics*, 5, 39-64.

Formatted: Spanish (Mexico)

Formatted: Spanish (Mexico)

Formatted: Spanish (Mexico)

Formatted: Spanish (Mexico)

- 776 Marchant, R. et al., 2002. Distribution and ecology of parent taxa of pollen lodged within the Latin  
777 American Pollen Database. *Review of Palaeobotany and Palynology*, 121, 1-75.
- 778 Méndez Linares, A., López-Portillo, J., Hernández-Santana, J., Pérez, M.O., Orozco, O.O.J.C., 2007.  
779 The mangrove communities in the Arroyo Seco deltaic fan, Jalisco, Mexico, and their  
780 relation with the geomorphic and physical-geographic zonation. *70*, 127-142.
- 781 Metcalfe, S.E., O'Hara, S.L., Caballero, M., Davies, S.J., 2000. Records of Late Pleistocene-Holocene  
782 climate change in Mexico- a review. *Quaternary Science Reviews*, 19, 699-721.
- 783 Meyers, P.A., 1997. Organic geochemical proxies of paleoceanographic, paleolimnologic, and  
784 paleoclimatic processes. *Organic geochemistry*, 27, 213-250.
- 785 Milliken, K., Anderson, J.B., Rodriguez, A.B., 2008. A new composite Holocene sea-level curve for  
786 the northern Gulf of Mexico. *Geological Society of America Special Paper*, 443, 1-11.
- 787 Moreno-Casasola, P., 2006. Entornos veracruzanos: la costa de La Mancha, Instituto de Ecología,  
788 A.C., Xalapa, Veracruz, Mexico.
- 789 Mueller, A.D. et al., 2010. Late Quaternary palaeoenvironment of northern Guatemala: evidence  
790 from deep drill cores and seismic stratigraphy of Lake Petén Itzá. *Sedimentology*, 57, 1220-  
791 1245.
- 792 Parkinson, R.W., DeLaune, R.D., White, J.R., 1994. Holocene sea-level rise and the fate of  
793 mangrove forests within the wider Caribbean region. *Journal of Coastal Research*, 1077-  
794 1086.
- 795 Ramírez-Marcial, N., González-Espinosa, M., Williams-Linera, G., 2001. Anthropogenic disturbance  
796 and tree diversity in montane rain forests in Chiapas, Mexico. *Forest Ecology  
797 Management*, 154, 311-326.
- 798 Ranwell, D.S., 1972. Ecology of salt marshes and sand dunes, *Ecology of salt marshes and sand  
799 dunes*. Chapman and Hall, London, pp. 200 pp.
- 800 Reimer, P.J. et al., 2013. IntCal13 and Marine13 radiocarbon age calibration curves 0–50,000 years  
801 cal BP. *Radiocarbon*, 55, 1869-1887.
- 802 Renssen, H. et al., 2009. The spatial and temporal complexity of the Holocene thermal maximum.  
803 *Nature Geoscience*, 2, 411-414.
- 804 Richardson, D.M., 1998. *Ecology and Biogeography of Pinus*. Cambridge University Press,  
805 Cambridge.
- 806 Rzedowski, J., 2006. *Vegetación de México*. Comisión Nacional para el Conocimiento y Uso de la  
807 Biodiversidad, México D.F., pp. 504 pp.
- 808 Servicio Meteorológico Nacional, 2018. Normales climatológicas, Estado de Veracruz, Estación La  
809 Mancha (online, last accessed June 2018).
- 810 Soares, M., 2009. A conceptual model for the responses of mangrove forests to sea level rise.  
811 *Journal of Coastal Research*, 267-271.
- 812 Suárez, J.A., Urrego, L.E., Osorio, A., Ruiz, H.Y., 2015. Oceanic and climatic drivers of mangrove  
813 changes in the Gulf of Urabá, Colombian Caribbean. *Latin American Journal of Aquatic  
814 Research*, 43.
- 815 Thom, B.G., 1967. Mangrove ecology and deltaic geomorphology: Tabasco, Mexico. *The Journal of  
816 Ecology*, 301-343.
- 817 Thorhaug, A., Poulos, H.M., López-Portillo, J., Ku, T.C., Berlyn, G., 2017. Seagrass blue carbon  
818 dynamics in the Gulf of Mexico: Stocks, losses from anthropogenic disturbance, and gains  
819 through seagrass restoration. *Science of The Total Environment*, 605, 626-636.
- 820 Toscano, M.A., Macintyre, I.G., 2003. Corrected western Atlantic sea-level curve for the last 11,000  
821 years based on calibrated 14C dates from *Acropora palmata* framework and intertidal  
822 mangrove peat. *Coral reefs*, 22, 257-270.

Formatted: Spanish (Mexico)

Formatted: English (United States)

Formatted: Spanish (Mexico)

Formatted: English (United States)

Formatted: Spanish (Mexico)

- 823 | Travieso-Bello, A., 2000. Biodiversidad del paisaje costero de La Mancha, Actopan, Veracruz.  
824 | Instituto de Ecología, Xalapa.
- 825 | Urrego, L.E., Bernal, G., Polanía, J., 2009. Comparison of pollen distribution patterns in surface  
826 | sediments of a Colombian Caribbean mangrove with geomorphology and vegetation.  
827 | Review of Palaeobotany and Palynology, 156, 358-375.
- 828 | Urrego, L.E., Correa-Metrio, A., González, C., Castaño, A.R., Yokoyama, Y., 2013. Contrasting  
829 | responses of two Caribbean mangroves to sea-level rise in the Guajira Peninsula  
830 | (Colombian Caribbean). Palaeogeography, Palaeoclimatology, Palaeoecology, 370, 92-102.
- 831 | Urrego, L.E., Correa-Metrio, A., González-Arango, C., 2018. Colombian Caribbean mangrove  
832 | dynamics: anthropogenic and environmental drivers. Boletín de la Sociedad Geológica  
833 | Mexicana, 70, 133-145.
- 834 | Urrego, L.E., González, C., Urán, G., Polanía, J., 2010. Modern pollen rain in mangroves from San  
835 | Andres Island, Colombian Caribbean. Review of Palaeobotany and Palynology, 162, 168-  
836 | 182.
- 837 | Valiela, I., Bowen, J.L., York, J.K., 2001. Mangrove Forests: One of the World's Threatened Major  
838 | Tropical Environments. Bioscience, 51, 807-815.
- 839 | Vovides, A.G. et al., 2014. Morphological plasticity in mangrove trees: salinity-related changes in  
840 | the allometry of *Avicennia germinans*. Trees, 28, 1413-1425.
- 841 | Ward, R.D., Friess, D.A., Day, R.H., MacKenzie, R.A., 2016. Impacts of climate change on mangrove  
842 | ecosystems: a region by region overview. Ecosystem Health Sustainability, 2, e01211.
- 843 | Williams-Linera, G., 2002. Tree species richness complementarity, disturbance and fragmentation  
844 | in a Mexican tropical montane cloud forest. Biodiversity & Conservation, 11, 1825-1843.
- 845 | Wooller, M.J., Morgan, R., Fowell, S., Behling, H., Fogel, M., 2007. A multiproxy peat record of  
846 | Holocene mangrove palaeoecology from Twin Cays, Belize. The Holocene, 17, 1129-1139.
- 847 | Zar, J.H., 1999. Biostatistical Analysis. 4th ed. Prentice-Hall, Upper Saddle River, NJ.

848

Formatted: English (United States)

1 **Holocene establishment of mangrove forests in the western coast of the Gulf of Mexico**

2

3 Cordero-Oviedo, C<sup>a</sup>, A. Correa-Metrio<sup>b,\*</sup>, L.E. Urrego<sup>c</sup>, G. Vázquez-Hurtado<sup>d</sup>, M.

4 Blaauw<sup>e</sup>, J. Escobar<sup>f,g</sup>, J.H. Curtis<sup>h</sup>

5 <sup>a</sup> Posgrado en Ciencias de la Tierra, Universidad Nacional Autónoma de México,  
6 Coyoacán, Ciudad de México, México 04510, [ceciliacorderoviedo@gmail.com](mailto:ceciliacorderoviedo@gmail.com), <sup>b</sup>  
7 Instituto de Geología, Universidad Nacional Autónoma de México, Coyoacán,  
8 Ciudad de México, México 04510, [acorrea@geologia.unam.mx](mailto:acorrea@geologia.unam.mx), <sup>c</sup> Departamento de  
9 Ciencias Forestales, Universidad Nacional de Colombia, Sede Medellín A.A. 568  
10 Medellín, Colombia, [leurrego@unal.edu.co](mailto:leurrego@unal.edu.co), <sup>d</sup> Instituto de Ecología, A.C. Carretera  
11 antigua a Coatepec 351, El Haya, Xalapa 91070, Veracruz, México,  
12 [gabriela.vazquez@inecol.mx](mailto:gabriela.vazquez@inecol.mx), <sup>e</sup> School of Natural and Built Environment, Queen's  
13 University Belfast, Belfast, United Kingdom, [maarten.blaauw@qub.ac.uk](mailto:maarten.blaauw@qub.ac.uk), <sup>f</sup>  
14 Departamento de Ingeniería Civil y Ambiental, Universidad del Norte, Km 5 Via Puerto  
15 Colombia, Colombia, [jhescobar@uninorte.edu.co](mailto:jhescobar@uninorte.edu.co), <sup>g</sup> Center for Tropical Paleocology and  
16 Archaeology, Smithsonian Tropical Research Institute, Box 0843-03092, Balboa, Panama, <sup>h</sup>  
17 Department of Geological Sciences, University of Florida, Gainesville, FL, 32611, USA,  
18 [curtisj@ufl.edu](mailto:curtisj@ufl.edu)

19

20 **\*Corresponding autor:** Alexander Correa-Metrio, [acorrea@geologia.unam.mx](mailto:acorrea@geologia.unam.mx)

21

22 **Abstract**

23 The successful establishment of mangrove ecosystems depends on an intricate network of  
24 interactions among physical and biological factors that are highly dynamic through time. At  
25 millennial to centennial time scales, regional climates, sea levels, and local geomorphology

26 play critical roles in the establishment of mangroves. Whereas fluvio-marine dynamics  
27 define coastal sedimentary settings, regional precipitation and freshwater input modulate  
28 salinity and seasonal flooding patterns. We analyzed a ~7800-year-old, continuous  
29 sedimentary record from the western coast of the Gulf of Mexico to shed light on regional  
30 biophysical coastal processes and the history of the mangroves that occupy the region  
31 today. We used a systematic sampling of mud-water interface sediments to generate a  
32 modern reference frame for interpreting fossil pollen assemblages. Our results indicate that  
33 the cored location that is currently approximately at sea level, was below sea level from  
34 ~7800 to 4000 calibrated years before present (cal BP). The establishment of dense  
35 mangrove stands took place around 3700 cal BP, when regional sea levels stabilized,  
36 resulting in a substantial increase of organic matter and therefore carbon stored in the  
37 sediments. However, the mangrove ecological succession that started at ~6000 cal BP was  
38 interrupted by a regional drought that extended from ~5400 to 3700 cal BP. From 3700 cal  
39 BP to Present, the lagoon has been characterized by relatively stable both substratum and  
40 sea level, that together have facilitated the establishment of mangrove forests. Overall, our  
41 record demonstrates the complexity of the interactions between local and regional factors in  
42 the development and evolution of both coastal geomorphology and ecosystems.

43

44 Keywords: coastal environment; Gulf of Mexico; Holocene; mangroves; sea-level changes;  
45 pollen analysis

46

47 **1. Introduction**

48 Mangrove ecosystems are a large component of tropical and sub-tropical coastal  
49 landscapes. Occupying intertidal zones (Lugo and Snedaker, 1974), they regulate the  
50 relationship between continental discharge of sediments and water and sea level (Ellison,  
51 1989). The main engineers of these ecosystems are a reduced group of plant species  
52 physiologically adapted to brackish-to-saline substrates (Ball, 2002; Vovides et al., 2014).  
53 The establishment of mangrove forests creates the conditions for complex food webs that  
54 incorporate marine and continental components. The entire mangrove ecosystem is  
55 fundamental for providing products and ecological services, resulting in direct and indirect  
56 uses by human populations, mainly fuelwood, fisheries, sediment trapping, and carbon  
57 storage (Bouillon et al., 2008; Feller et al., 2017; Méndez et al., 2007; Ward et al., 2016).

58         Although they represent one of the most important carbon sinks worldwide  
59 (Bouillon et al., 2008), together with coral reefs and tropical forests, mangroves are among  
60 the most endangered modern ecosystems (Valiela et al., 2001). It has been estimated that  
61 through the last two decades of the 20th Century, 35% of the global mangrove area had  
62 been lost mostly because of direct and/or indirect anthropogenic causes (FAO, 2007). The  
63 main human-related causes of mangroves loss are the conversion to aquaculture and  
64 agriculture, urbanization, and pollution (Feller et al., 2017; Gilman et al., 2008; Thorhauga  
65 et al., 2017), which in Mexico have translated in a net loss ~240 ha/year through the last  
66 decades (Hamilton and Cassey, 2016). The rapid rate at which these threats to mangrove  
67 ecosystems are growing highlights the need to understand them in the context of their  
68 natural history and the intricate network of factors that interact to facilitate or impede their  
69 colonization and establishment.



70           A wide variety of factors interact to create the specific conditions under which  
71 mangrove communities thrive and persist through time (Gilman et al., 2008). Healthy  
72 vigorous mangrove forests, and therefore ecosystems, depend on a delicate balance  
73 between marine influences and freshwater and sediment input from continental areas acting  
74 upon specific geomorphologic settings (Lugo and Snedaker, 1974; Soares, 2009). Whereas  
75 marine influences on mangrove ecosystems materialize through tidal regimes and sea level  
76 changes that define baseline for erosion and accumulation of sediments, regional climates  
77 and vegetation cover over the mainland control continental discharge of freshwater and  
78 sediments along the coast. Thus, through the Holocene, changes in precipitation, vegetation  
79 cover, geomorphologic dynamics, and sea levels have probably led to high environmental  
80 variability over the intertidal areas (Geissert Kientz, 1999). In the Gulf of Mexico and the  
81 Caribbean, regional sea levels have progressively risen since the deglaciation (Milliken and  
82 Anderson, 2008; Toscano and Macintyre, 2003), whereas annual precipitation has shown a  
83 wide variability associated with extraterrestrial forcings (e.g. solar activity and orbital  
84 cycles, Haug et al. 2001, Hodell et al. 2001) and higher frequency processes associated with  
85 complex internal systems (e.g. El Niño-Southern Oscillation, Moy et al. 2002). The balance  
86 between fluvial loads and sea-level rise modulates local geomorphologic and sedimentary  
87 processes, defining the formation of either depositional or erosional environments the  
88 balance of which is in turn critical for the establishment and persistence of mangroves  
89 (Parkinson et al., 1994). Indeed, modern net losses of mangrove cover have been widely  
90 associated with sea-level rises along unprotected coasts (Suárez et al., 2015). Thus, the  
91 definition of the context that led to the development of modern mangrove forests would  
92 provide important clues for identifying the limits of environmental pressure that these  
93 ecosystems can endure.

94 Sedimentary deposits that accumulate in coastal lagoons provide a natural record of  
95 the evolution of coastal landscapes through time. Understanding the natural development of  
96 mangrove ecosystems and the main factors involved in the process would give insights into  
97 the threat level that coastal zones face given modern environmental change (Lopez-Portillo  
98 et al., 2011; Thom, 1967). Here we use the pollen record of a 13-m-long ~8,000-year-old  
99 sedimentary sequence retrieved from La Mancha Lagoon, State of Veracruz, Mexico, to  
100 reconstruct the history of the local vegetation through the Holocene. By analyzing the  
101 history of vegetation assemblages as reflected by fossil pollen spectra, we aim to answer  
102 the following questions: i) what has been the role of sea-level rise and precipitation  
103 variability through the Holocene in the establishment and persistence of mangrove forests  
104 in the west coastline of the Gulf of Mexico? ii) when did the barrier-lagoon systems of the  
105 region consolidate in the context of Holocene environmental variability?

106

## 107 **2. Study Area**

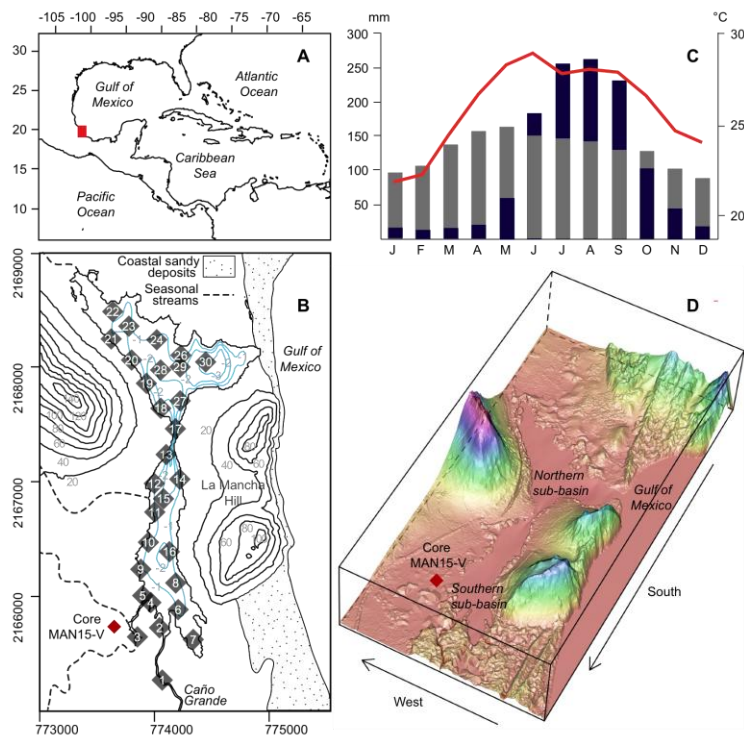
108 La Mancha lagoon is located in the State of Veracruz, Mexico, on the western  
109 coasts of the Gulf of Mexico (19.579 N°, 96.387 W°, Fig. 1). With a north-to-south length  
110 of 3 km, the lagoon has an area of ~1.35 km<sup>2</sup> distributed in two sub-basins separated by a  
111 strait located near the center of the water body (Fig. 1). Whereas the southern sub-basin is  
112 exposed to permanent freshwater input from the Caño Grande River that drains water from  
113 a basin of almost 2,500 km<sup>2</sup>, the northern sub-basin more exposed to tidal influence  
114 through an ephemeral mouth that communicates seasonally with the sea (Fig.1) (Lankford,  
115 1977; Moreno-Casasola, 2006). During the dry season, a sand bar accumulates closing the  
116 estuarine mouth and causing a damming of continental freshwater. With the onset of the

117 rainy season, freshwater starts to accumulate, eventually breaking the sandbar, opening the  
118 mouth, and creating a direct connection with the sea (Moreno-Casasola, 2006). Thus,  
119 lagoon dynamics are intimately linked to regional climate that is warm (temperatures from  
120 22 to 26 °C), with an annual mean precipitation of 1222 mm, with 85% of the annual value  
121 falling between June and October (Fig. 1) (Servicio Meteorologico Nacional, 2018). The  
122 dry season is especially pronounced between December and April with mean monthly  
123 precipitation below 20 mm, while November and May are characterized by a mean  
124 precipitation around 50 mm. By the end of the summer and early autumn, the area is  
125 exposed to tropical cyclones, although their incidence is relatively low compared with other  
126 areas of the Gulf of Mexico (Moreno-Casasola, 2006).

127         La Mancha lagoon belongs to a geomorphic unit known as the Low Cumulative  
128 Plain that formed during the Quaternary (Geissert Kientz, 1999), allowing deposition of  
129 clayey-silt sediments. The lagoon formed at the margin of a volcanic mountain range that  
130 interrupts the coastal plain of the Gulf of Mexico (Geissert Kientz, 1999; Fig. 1). The  
131 current morphology of the area has been mostly shaped by Quaternary dynamics, going  
132 from an empty deep basin during times of sea-level low stands to a depositional coastal  
133 plain during times of sea-level high stands (Geissert Kientz, 1999; Kjerfve, 1994). The  
134 mountain ridge that connects La Mancha Hill with the adjacent western mountains divides  
135 La Mancha lagoon into two contrasting sub-basins (Fig. 1). Differences in freshwater input,  
136 marine influence, and energy of the sedimentary environments have created two clearly  
137 distinct environments for mangrove forests, which today occupy ~3.55 km<sup>2</sup> around the  
138 lagoon.

139         Regional tides are mixed, mostly diurnal and of low amplitude (highest and lowest  
140 tidal levels at 22 cm and -30 cm from average sea level, respectively), preventing the

141 formation of tidal currents. This feature together with the permanent input of fresh water  
 142 and the sheltering of the lagoon from the energy of the waves by La Mancha Hill (Fig. 1)  
 143 have probably played a critical role in maintaining the morphology of the lagoon, avoiding  
 144 the formation of tidal mudflats, marshes, and/or estuaries (Geissert Kientz, 1999). Over  
 145 recent decades, progressive loss of depth of the lagoon because of sediment accumulation  
 146 suggests that sediment input surpasses local erosion (Moreno-Casasola, 2006), although  
 147 this might not have been the case through the entire history of the area.



148  
 149 Figure 1. Study area. A. Location of La Mancha lagoon in the continental context. B.  
 150 Locations sampled for modern and fossil sediments in the local context of La Mancha  
 151 coastal lagoon; elevation contours are shown in increments of 20 m asl (solid black lines),  
 152 whereas a basic bathymetry based on field observations is shown as blue contours. C.  
 153 Monthly precipitation (blue bars), evapotranspiration (gray bars), and monthly mean

154 temperature (black line with dots) at La Mancha Meteorological Station (Servicio  
155 Meteorológico Nacional, 2018) D. Topographic representation of La Mancha coastal  
156 lagoon.

157

158           Pollen assemblages contained in sediments reflect parental vegetation and are  
159 therefore useful for reconstructing environmental dynamics through time (e.g. Carrillo-  
160 Bastos et al., 2010; Urrego et al., 2009; Urrego et al., 2018). Given the regional  
161 geomorphology, the large size of the catchment basin of Caño Grande River, and the  
162 proximity to high mountain ranges, the pollen spectra of sediments from La Mancha lagoon  
163 contains regional and local taxa (Moreno-Casasola, 2006; Travieso-Bello, 2000). Whereas  
164 the former are transported by water and wind currents, the latter are produced by *in situ*  
165 vegetation (Hooghiemstra et al., 2006). Regional elements come mostly from montane  
166 forests that dominate the regional highlands (Rzedowski, 2006; Williams-Linera, 2002) and  
167 are characterized by wind-pollinated taxa with long-distance pollen dispersal (e.g. *Alnus*,  
168 *Myrica*, Ulmaceae, *Quercus*, and *Pinus*), which tend to be overrepresented in the pollen  
169 spectra. From within these allochthonous elements, *Pinus* is worth noticing because of the  
170 opportunist nature of most of the parental species (Richardson, 1998), which results in a  
171 high representation of this taxon in pollen spectra when environmental conditions are  
172 suboptimal for other arboreal elements (e.g. during droughts, Correa-Metrio et al., 2013).  
173 Local elements of the pollen spectra are in turn associated with two main vegetation types,  
174 namely lowland and mangrove forests. The hills that surround the lagoon reach heights up  
175 to 300 m asl and are mostly occupied by species of *Desmodium*, *Inga*, *Machaerium*,  
176 *Psychotria*, *Protium*, *Bursera*, Moraceae-Urticaceae and *Acacia*. The salt marshes, coastal  
177 dunes, and beaches that characterize flood plains are mainly dominated by species of

178 Cyperaceae, Amaranthaceae, *Typha*, Asteraceae, Chenopodiaceae, *Mimosa* and *Croton*.

179 These vegetation types can be associated with the distal part of a marine transgression  
180 plain, or be related to the first stage of a progradational pattern indicative of a typical  
181 ecological succession on intertidal habitats (González and Dupont, 2009).

182         The edges of the lagoon are occupied by species typical of mangrove forests,  
183 *Rhizophora mangle*, *Avicennia germinans*, *Conocarpus erectus* and *Laguncularia*  
184 *racemosa* (Travieso-Bello, 2000). The interplay of these species is modulated by their  
185 differential adaptation to the changing environmental conditions along a salinity gradient,  
186 which in turn defines the structure and composition of the forest (Lugo and Snedaker, 1974;  
187 Travieso-Bello, 2000; Urrego et al., 2009). Thus, these forests are highly sensitive to  
188 changes in sea-level, coastal progradation and/or erosion at different time scales (Ellison,  
189 2008). Mangrove forest species are adapted to specific environmental conditions, with *R.*  
190 *mangle* tolerating high inundation levels, strong wave energy and shorter distances to the  
191 sea, *A. germinans* thriving in more saline environments, hurricane-disturbed or  
192 experiencing severe droughts, *L. racemosa* being restricted to average minimum  
193 temperatures over 15.5 °C and successional processes triggered by anthropogenic  
194 disturbance, and *C. erectus* being tolerant to higher sediment pH typical of supra-tidal  
195 waters close to well drained forests (González et al., 2010; Hogarth, 2007; Urrego et al.,  
196 2009; Urrego et al., 2010).

197         Regional human occupation has been reported since at least ~4,600 BP, and the  
198 lagoon has apparently been an important source of resources for human populations  
199 (Moreno-Casasola, 2006). This factor has exerted direct pressure on the mangrove forest  
200 through deforestation for timber and fuel wood extraction, and more recently in the  
201 interruption of surface and subsurface flows in the by infrastructure of the oil industry.

202 These local factors have been especially harsh on the northern sub-basin, where only sparse  
203 remnants of the mangrove forest survive today. Thus, whereas vigorous mangrove forests  
204 surround the southern sub-basin, the northern sub-basin is occupied by highly disturbed  
205 vegetation including sparse mangrove remnants. Regionally, growing human population  
206 and the parallel development of infrastructure apply further pressures to coastal ecosystems  
207 through pollution, accelerated erosion, increasing sea level, among other elements (Gilman  
208 et al., 2008).

209

### 210 **3. Methods**

#### 211 *3.1 Field work and laboratory analysis*

212 In autumn 2015, a 13-meter-long core was recovered from the southern part of La Mancha  
213 coastal lagoon (core MAN15V, Fig. 1), under an *A. germinans* stand, using a modified  
214 Livingston piston corer (Colinvaux et al., 1999). The core was longitudinally sectioned,  
215 stratigraphically described, and stored at ~ 4°C to preserve the sedimentary evidence. The  
216 chronological control of the sedimentary sequence was based on eight accelerator-mass-  
217 spectrometer (AMS) radiocarbon dates of bulk sediment, given that no other material such  
218 as macrofossils or charcoal could be found. Radiocarbon dates were calibrated to years  
219 before present (hereafter cal BP) using the IntCal13 curve (Reimer et al., 2013), and  
220 calibrated dates were used to build a Bayesian age-depth model using Bacon (Blaauw and  
221 Christen, 2011). The core was subsampled every ~ 12.5 cm for pollen analysis, aiming at a  
222 temporal resolution of ~75 years between contiguous samples. A total of 104 samples were  
223 processed for pollen analysis using standard pollen extraction techniques (Faegri and  
224 Iversen, 1989). Samples were analyzed under transmitted-light microscope at

225 magnifications of x400 and x1000, aiming to reach a minimum pollen sum of 300 pollen  
226 grains. Grains of the family Cyperaceae and pteridophytes spores were excluded from the  
227 pollen sum, although they were counted and included in the interpretation. Pollen counts  
228 were transformed into percentages of the pollen sum and a stratigraphic pollen diagram was  
229 constructed.

230           Pollen taxa were classified into five groups according to their modern ecological  
231 affinities (ecological affinities after Lugo and Snedaker 1974, Ranwell 1972, Travieso-  
232 Bello 2000): i) mangroves represented by *Rhizophora mangle*, *Avicennia germinans*, and  
233 *Conocarpus erectus*; although *Laguncularia racemosa* is an important component of the  
234 local mangrove forests, it was not found in the pollen spectra; ii) salt marsh vegetation  
235 represented by Cyperaceae, Amaranthaceae, *Croton*, *Typha*, Asteraceae, Chenopodiaceae,  
236 and *Mimosa*; iii) lowland forest represented by *Inga*, *Acacia*, *Machaerium*, *Protium*,  
237 *Bursera*, and Moraceae-Urticaceae; iv) montane regional forests represented by *Alnus*,  
238 *Myrica*, Ulmaceae, *Quercus*, and *Miconia*; and v) disturbance taxa represented by *Pinus*  
239 and Poaceae; these latter taxa were classified as representatives of disturbance because in  
240 Mexico they are distributed along environments unfavorable to vegetation development,  
241 usually associated with either natural or anthropogenic causes (Franco-Gaviria et al., 2018;  
242 Rzedowski, 2006). High abundances of *Pinus* pollen have been reported for areas subjected  
243 to dry conditions and/or regimes of high disturbance (Correa-Metrio et al., 2013; Metcalfe  
244 et al., 2000), mostly associated with early succession colonizers (Ramirez-Marcial et al.,  
245 2001). Meanwhile, although Poaceae pollen is characteristic of successional processes of  
246 supratidal plains (Bush, 2002; Urrego et al., 2013), it is also found in pollen assemblages



247 from all Mexican vegetation types, usually associated with disturbance (Correa-Metrio et  
248 al., 2013; Franco-Gaviria et al., 2018).

249 The fossil pollen record was complemented by sampling 30 locations  
250 homogeneously for modern mud-water interface (15 samples from each sub-basin)  
251 distributed across the water body, using an Ekman dredge. This sampling was meant to  
252 cover the variability of the modern pollen spectra (Fig.1), especially the differences  
253 between depositional environments of the two sub-basins. Samples were treated and  
254 analyzed using the same techniques as the fossil samples.

255 Total both C (%TC) and N (%TN) were measured in fossil samples every 5 cm  
256 along the core and in modern samples. For this purpose, samples were freeze dried and  
257 crushed, and subsequently analyzed using a Carlo Erba NA1500 CNS elemental analyzer.  
258 Additionally, coulometric titration was used to determine carbonate carbon (%TIC) in  
259 modern samples, allowing the estimation of organic carbon (%TOC). The discrimination of  
260 TC into TIC and TOC in modern samples was used to infer the relationship between these  
261 two carbon sources in the system of La Mancha lagoon.

262

### 263 *3.2 Statistical Analysis*

264 A non-metric multidimensional scaling ordination (NMDS) was applied on pollen relative  
265 abundances, including both modern and fossil samples. The ordination was performed to  
266 summarize the temporal variability of the pollen spectra, and to evaluate vegetation  
267 temporal dynamics in the context of the modern lagoon. This technique ordines samples  
268 on a  $k$ -dimensional space defined *a priori* by the analyst, aiming to maintain the original

269 topologic relationships among samples (Legendre and Legendre, 2012). Although two-  
270 dimensional ordinations are readily used, we selected three dimensions to produce a relaxed  
271 ordination where the affinity among pollen spectra can manifest more freely. We used the  
272 Bray-Curtis metric to estimate dissimilarity among samples, a metric that relies more on  
273 compositional data than on the abundance of individual taxa and has been proven  
274 monotonic to ecological distance (Faith et al., 1987).

275         Modern samples were classified into southern and northern sub-basins as  
276 representative of dense and sparse mangrove forests, respectively. Whereas the northern  
277 sub-basin has direct contact with the sea through the ephemeral mouth, which creates a  
278 more energetic environment, and has been subjected to important human disturbances and  
279 modifications resulting in sparse mangrove cover, the southern sub-basin is more  
280 influenced by the entrance of the river and is occupied by a well-developed dense  
281 mangrove stand. Thus, pollen spectra from these two sub-basins should reflect contrasting  
282 mangrove-forest cover conditions, and their relative oceanic and fluvial influences. The  
283 statistical significance of the difference between NMDS sample scores of the two sub-  
284 basins were tested using a two-sample t-test (Zar, 1999). TIC, TOC, TC, and TN content in  
285 modern samples were compared using Pearson correlation coefficient, whereas  
286 comparisons of concentrations between the northern and southern sub-basins were also  
287 compared using two-sample t-test (Zar, 1999).

288

## 289 **4. Results**

### 290 *4.1 Stratigraphy and chronology of the sedimentary record*

291 Sediments from the La Mancha coastal lagoon were mostly brownish, shelly clays with low  
292 content of organic material, and some intermissions of brownish silt with shell fragments  
293 and organic material (Fig. 2A). From the base of the core up to 1200 cm below lagoon floor  
294 (blf hereafter), the sediments were brown shelly clay, while from 1200 to 663 cm blf the  
295 color turned into a light brown matrix (clay and silt) with shell fragments and carbonates.  
296 From 663 to 615 cm blf the clayey sediment was brown with light brown bands. From 615  
297 to 372 cm blf, the sediment showed brownish tones, and were mostly composed of clay  
298 with a thin layer of silt, shelly and little organic material. The uppermost 327 cm were dark  
299 to very light brown, with a uniform shelly clay composition (Fig 2A).

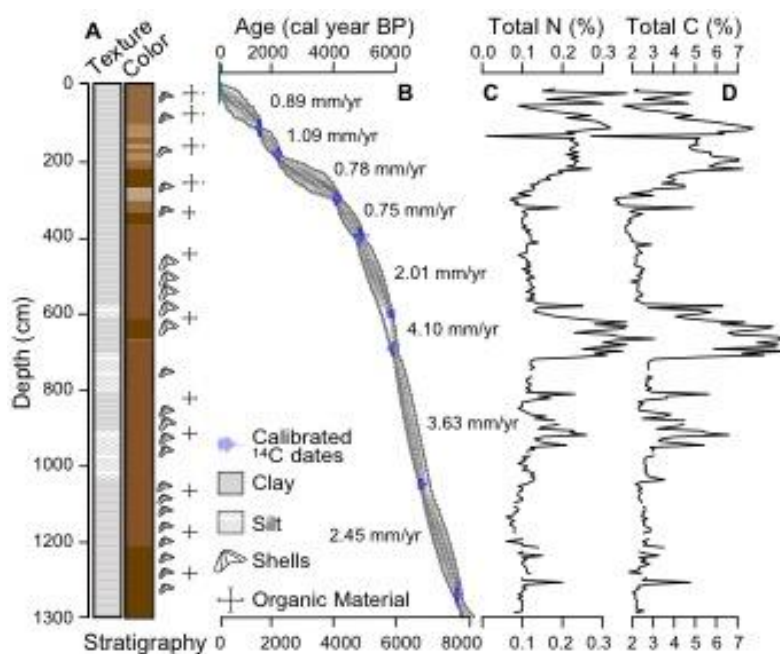
300 All radiocarbon dates resulted in stratigraphic order (Table 1). Although bulk  
301 sediment dates could lead to an  $^{14}\text{C}$  age offset, we were not able to quantify it because of  
302 the lack of other quantifiable materials. Nevertheless, the high correspondence between TC  
303 and TN along the sedimentary record (Fig. 2) suggests that inorganic carbon represents a  
304 relatively low proportion of the sedimentary material. According to the age-depth model,  
305 the core has a basal age of  $\sim 7840$  cal BP, resulting in an average sedimentation rate of 1.96  
306 mm/yr (Fig 2B). From the bottom of the sequence up to 5500 cal BP, sedimentation rates  
307 were high, with maximum values around 5500 cal BP (4.10 mm/yr). From c. 5500 cal BP  
308 to present, sedimentation rates showed a decreasing trend, reaching 0.89 mm/yr in the  
309 uppermost part of the core (Fig 2).

310

311 Table 1. Radiocarbon dates of core MAN15V from La Mancha coastal lagoon. Depths in  
312 cm below lagoon floor (blf). Ages calibrated after the IntCal13 curve (Reimer et al., 2013).

Laboratory code	Depth (cm blf)	<sup>14</sup> C Age	Error	Calibrated age (95% range; cal BP)
UBA-34340	109	1290	24	1181-1283
Beta-440367	175	1880	30	1730-1883
UBA-34341	282	3447	26	3637-3826
Beta-440368	373	3970	30	4300-4523
UBA-34342	564	4732	41	5326-5584
Beta-437078	649	4770	30	5334-5588
UBA-34343	979	5624	41	6312-6482
Beta-437079	1249	6700	30	7508-7616

313



314

315 Figure 2. Core MAN15V from La Mancha coastal lagoon. A. Stratigraphy of the  
 316 sedimentary sequence: texture (left), color (right), and organic and shell content. B. Age-  
 317 depth model; calibrated ages (blue silhouettes), 95% confidence intervals in grey (darker  
 318 colors indicate higher probability), and sedimentation rates (mm/yr). C and D. Percentage  
 319 of total nitrogen and total carbon content (TN and TC, respectively).

320

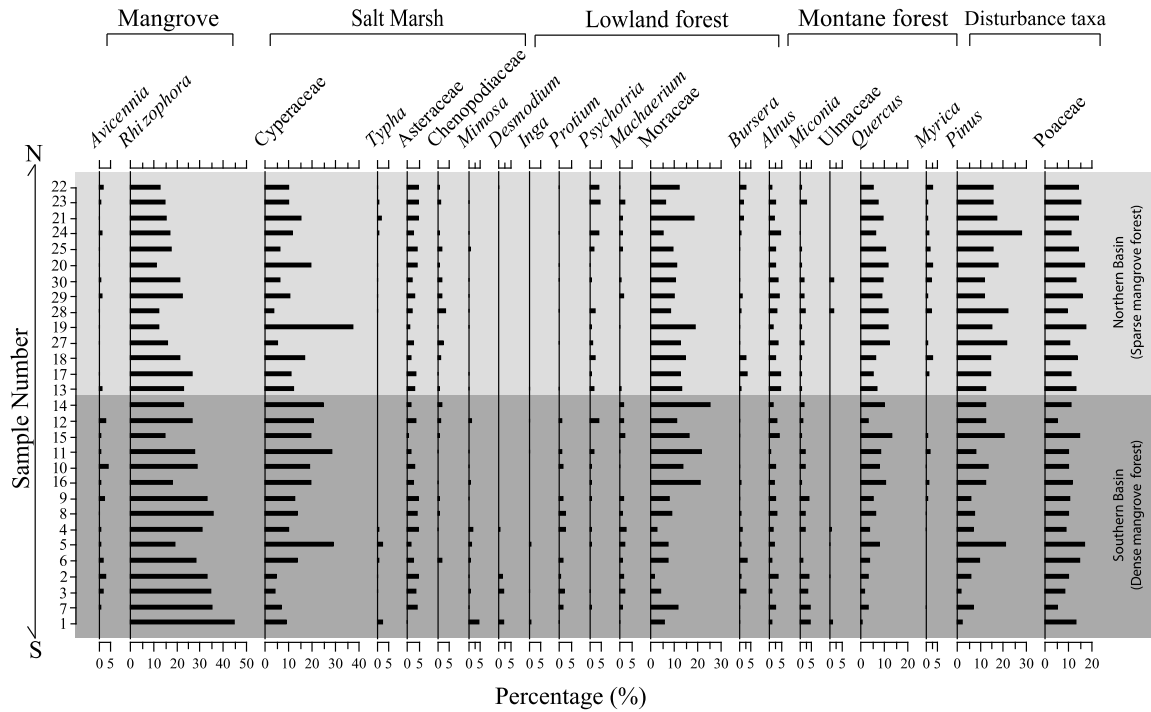
321 *4.2 Pollen spectra and C and N in modern samples*

322 Modern samples were characterized by 49 taxa, 18 and 31 identified at family and genus  
323 levels, respectively. Pollen sums varied between 300 and 387, whereas pollen counts  
324 including Cyperaceae and pterodophytes were between 322 and 472 palynomorphs.

325 *Rhizophora*, Cyperaceae, Moraceae-Urticaceae, *Quercus*, *Pinus*, and Poaceae dominated  
326 these samples (up to 45%), whereas taxa such as *Typha*, *Mimosa*, *Desmodium*, *Inga*, and  
327 Ulmaceae were poorly represented (less than 5%). One sample from the northern sub-basin  
328 was barren of pollen (sample 26, Fig. 1).

329 *Avicennia* and *Rhizophora* showed high percentages (up to 5 and 45%, respectively)  
330 towards the southern sub-basin of the lagoon (Figs. 1 and 3). Contrastingly, other taxa such  
331 as *Quercus*, *Myrica*, and *Pinus* decreased southwards. Compositional differences between  
332 the northern and southern sub-basins of the lagoon were also indicated by taxa that  
333 occurred only at the latter, such as *Desmodium*, *Inga*, and *Protium* (Figs. 1 and 3). Samples  
334 from the middle area of the lagoon (samples 12,13,14,17 and 18) (Figs. 1 and 3) contained  
335 the highest percentages of Cyperaceae and Moraceae-Urticaceae (25% and 30%,  
336 respectively), and minima of *Typha*, Asteraceae, and *Psychotria*. In the northern sub-basin  
337 (Figs. 1 and 3), *Quercus*, *Pinus*, and Poaceae dominated the pollen spectra with abundances  
338 above 10%.

339



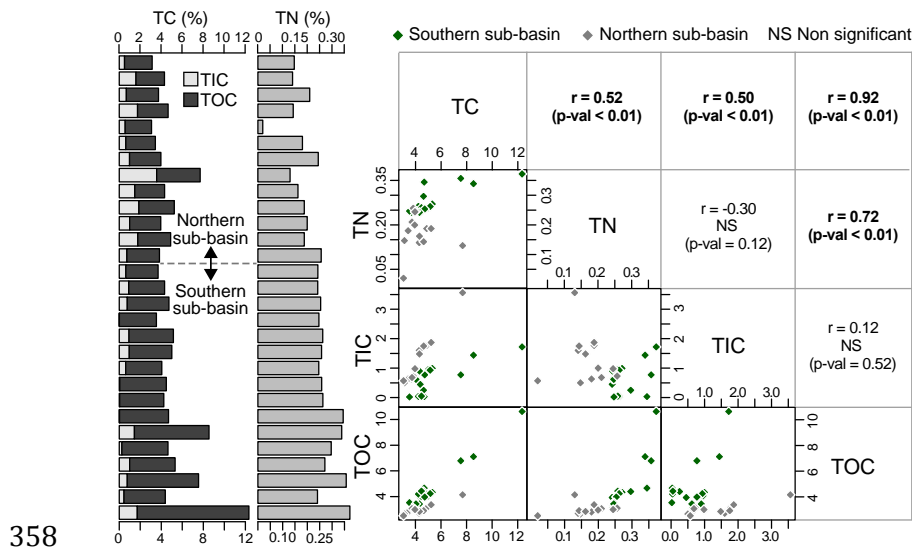
340

341 Figure 3. Pollen diagram of selected taxa from mud-water interface samples from La  
 342 Mancha coastal lagoon. Ecological affinities after Lugo and Snedaker (1974), Ramwell  
 343 (1972), and Travieso-Bello (2000). Samples are ordered from South to North with samples  
 344 from the southern (northern) sub-basin highlighted in dark (light) grey.

345

346 TC content in modern samples varied between 3.1 and 12.3%, with mean and median of 4.9  
 347 and 4.4%, respectively. Although mean values for the northern and southern sub-basins  
 348 were not statistically differentiable ( $t = 1.66$ ,  $p\text{-value} = 0.11$ ), the northern sub-basin  
 349 consistently showed lower values (Fig. 3). Differently, individual fractions of C resulted  
 350 statistically differentiable, with a higher concentration of TOC in the southern sub-basin  
 351 (3.56,  $p\text{-value} = 0.002$ ) and a higher concentration of TIC in the northern sub-basin ( $t =$   
 352 2.47,  $p\text{-value} = 0.023$ ). TN range between 0.02 and 0.37% with mean and median of 0.23

353 and 0.24%, respectively (Fig. 3), with higher mean concentration in the southern subbasin  
 354 ( $t = 5.54$ ,  $p$ -value  $< 0.001$ ). TC resulted statistically associated with TN, TIC, and TOC,  
 355 although the magnitude of the correlation was substantially higher with the latter (Fig. 3).  
 356 Whereas TIC resulted moderately associated only with TN, TOC was strongly associated  
 357 with both TC and TN (Fig. 3).



359 Figure 4. Content (%) of carbon and nitrogen in the modern samples of La Mancha coastal  
 360 lagoon. Total C content (TC) discriminated into inorganic and organic fractions (TIC and  
 361 TOC), and total N content (TN). Comparisons among sedimentary attributes are shown in  
 362 the right side panels (biplots and correlation coefficients with their significance).

363

#### 364 4.3 Fossil record

365 Fossil pollen types included 55 taxa classified into 24 families and 31 genera. Pollen sums  
 366 varied between 300 and 349 grains per sample (average 306 grains), whereas pollen counts  
 367 that included Cyperaceae and pterodophytes reached between 303 and 359 palynomorphs

368 per sample (average 317). The highest abundances were shown by *Rhizophora*, Moraceae-  
369 Urticaceae, *Quercus* and *Pinus*, while the lowest abundances were shown by *Conocarpus*,  
370 *Inga*, *Bursera* and *Miconia*. From within the 55 identified taxa, only *Rhizophora*,  
371 Cyperaceae, *Typha*, Asteraceae, Chenopodiaceae, Moraceae-Urticaceae, *Alnus*, *Quercus*,  
372 *Pinus*, and Poaceae persisted throughout the entire record. The record was discretized into  
373 four main pollen zones (Fig. 4) to facilitate the description of the sedimentary sequence.  
374 Pollen zones were defined based on an inspection of the distribution of pollen percentages  
375 through time, aiming to identify time periods characterized by relatively stable pollen  
376 assemblages.

377

378 **Pollen Zone I (from 1300 to 907 cm blf, c. 7840-6300 cal BP):** The sediment showed TC  
379 concentrations between 1.84 and 4.78%, with mean of 2.54%, and TN concentrations  
380 between 0.06 and 0.20%, with mean 0.10% (Fig. 2). This zone showed high percentages of  
381 *Rhizophora* (up to 20%), Moraceae-Urticaceae (up to 50%), *Quercus* (up to 20%), *Pinus*  
382 (up to 50%), and Poaceae (up to 20%). Low percentages (less than 5%) were shown by  
383 *Avicennia*, Amaranthaceae, *Croton*, *Typha*, Asteraceae, Chenopodiaceae, *Mimosa*, *Inga*,  
384 *Acacia*, *Machaerium*, *Protium*, *Bursera*, Ulmaceae and *Miconia* (Fig.4).

385

386 **Pollen Zone II (from 907 to 569 cm blf, c. 6300 - 5400 cal BP):** The sediment showed  
387 highly variable concentrations of both TC and TN (Fig. 2). TC varied between 2.28 and  
388 9.67% with mean of 4.6%, whereas TN varied between 0.09 and 0.43 with a mean of  
389 0.19%. This zone was dominated by Cyperaceae (20%), *Croton* (10%), *Typha* (20%),  
390 Chenopodiaceae (15%), Moraceae-Urticaceae (50%), *Alnus* (~6%), Ulmaceae (10%),  
391 *Quercus* (20%), *Pinus* (50%) and Poaceae (20%). Percentages below 5% were shown by



392 *Avicennia*, *Conocarpus*, Amaranthaceae, Asteraceae, *Mimosa*, *Inga*, *Machaerium*, *Protium*,  
393 *Bursera* and *Miconia* with less than 5%. The upper part of the zone was characterized by  
394 relatively low percentages of *Pinus* (~18%) and a substantial increase of Amaranthaceae,  
395 *Croton*, *Typha*, Asteraceae, Chenopodiaceae, and Cyperaceae (up to ~20%) (Fig. 4).

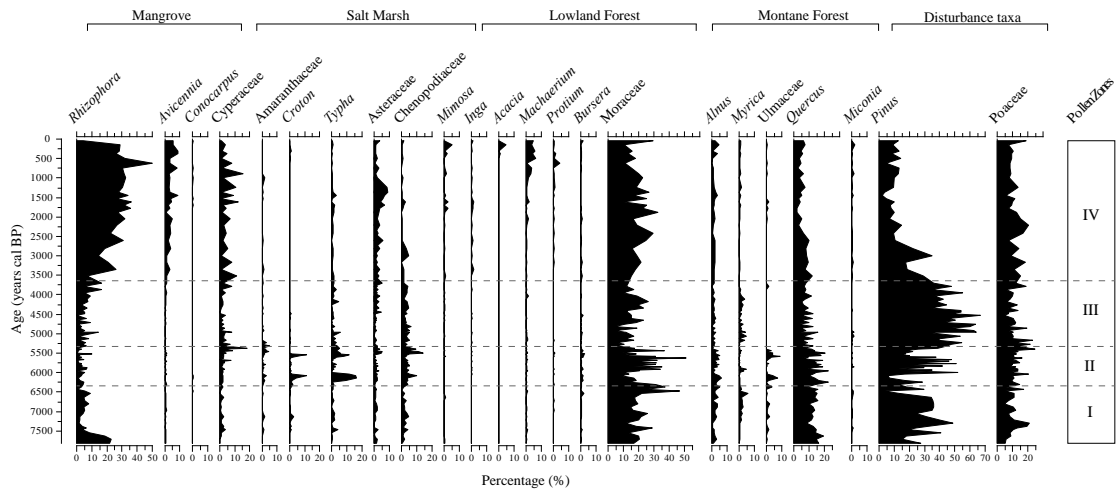
396

397 **Pollen Zone III (from 569 to 280 cm blf, c. 5400 - 3700 cal BP):** With lower variability,  
398 both TC and TN decreased substantially (Fig. 2). TC varied from 1.14 and 6.31% with  
399 mean of 2.45, and TN varied between 0.07 and 0.25% with mean of 0.12%. From 5400 BP  
400 *Rhizophora* abundances began to increase gradually, and *Avicennia* was less than 5%.  
401 *Pinus* reached the highest abundances throughout the record (up to 60%), while  
402 Amaranthaceae, *Croton*, *Mimosa*, *Inga*, *Machaerium*, *Bursera*, *Alnus*, Ulmaceae,  
403 Moraceae-Urticaceae, and *Miconia* showed their lowest percentages. Lastly, *Typha*,  
404 Asteraceae, and Chenopodiaceae showed abundances around 10% (Fig 4).

405

406 **Pollen Zone IV (from 280 to 0 cm blf, c. 3700 cal BP - Present):** TC and TN  
407 progressively reached high variable concentrations (Fig. 2). TC varied between 0.02 and  
408 7.77% with mean of 4.45%, and TN varied between 0.01 and 0.36% with mean of 0.20%.  
409 Abundances of *Rhizophora* and *Avicennia* reached their highest values (up to 60% and 10%  
410 respectively), and displayed an increasing trend towards the present. Amaranthaceae,  
411 *Croton*, *Typha*, Chenopodiaceae, *Myrica*, Ulmaceae, *Quercus*, and *Pinus* abundances  
412 decrease up to the present. Meanwhile *Acacia*, *Inga*, *Machaerium*, and *Protium* presented  
413 their highest abundances (up to 10%) (Fig. 4).

414



415

416 Figure 5. Fossil pollen diagram of selected taxa of core MAN15V from La Mancha coastal  
 417 lagoon. (ecological affinities after Lugo and Snedaker 1974, Ramwell 1972, and Travieso-  
 418 Bello 2000).

419

#### 420 4.4 Statistical analyses

421 The three-dimensional ordination of the modern and fossil pollen samples showed a stress  
 422 of 0.144. Negative scores along Axis 1 characterized modern samples, whereas fossil  
 423 samples were clearly divided into positive (negative) scores for samples older (younger)  
 424 than ~ 5400 cal BP (Fig. 5 and 6.B). Along Axis 2, both modern and fossil samples were  
 425 mostly located between -0.31 and 0.2, although fossil samples showed positive and  
 426 negative excursions (Fig. 5). NMDS Axis 3 was characterized by widespread scores for  
 427 fossil samples and almost exclusively negative scores for modern samples (Appendix 1).

428 The t-test for comparing NMDS scores of modern samples from the northern and  
 429 southern sub-basins yielded significant differences in terms of Axis 1 and 2, but non-  
 430 significant for Axis 3 (Table 2). Given the relatively flat behavior of Axis 2 and the lack of

431 significance of Axis 3 (Appendix 1), only the first axis of the ordination will be considered  
432 for interpretations hereafter.

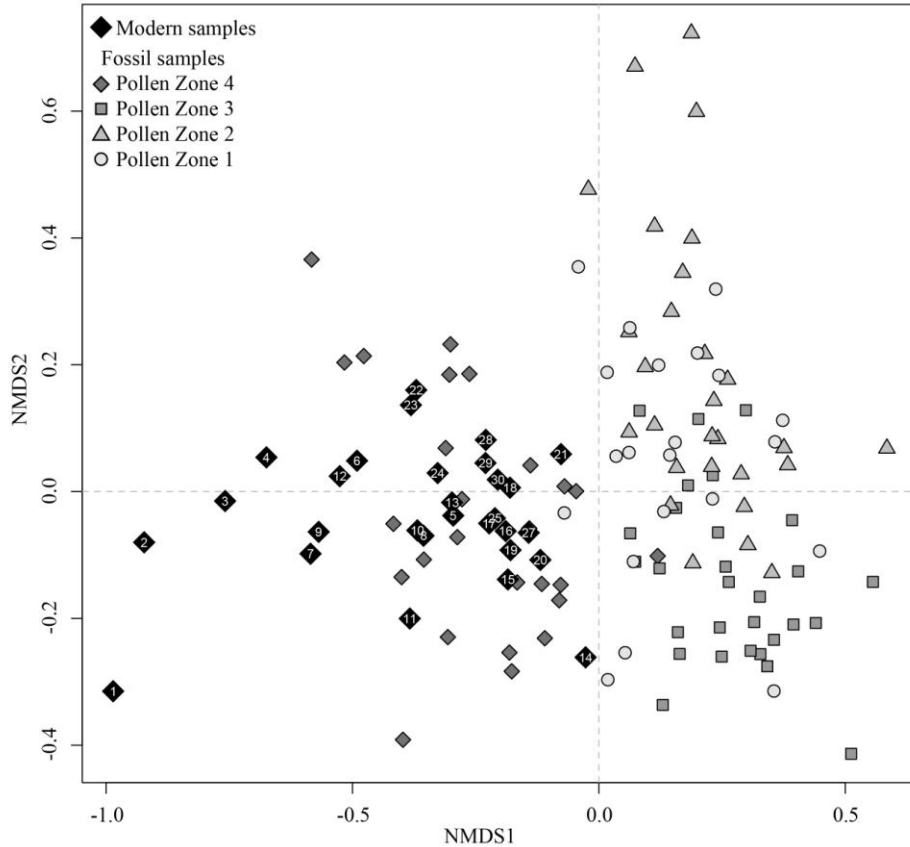
433

434 Table 2. Comparison of NMDS sample scores in the three axes for modern samples from  
435 the northern and southern sub-basins, i.e scores from dense (D) vs. sparse (S) mangrove  
436 areas. For the comparison of scores along each axis, t scores, degrees of freedom corrected  
437 for variance differences between samples (d.f.), and p-value are shown.

438

Comparison	t	d.f.	p-value
Axis 1 <sub>D</sub> – Axis 1 <sub>S</sub>	-3.5184	18	0.0026
Axis 2 <sub>D</sub> – Axis 2 <sub>S</sub>	-2.7661	26	0.0103
Axis 3 <sub>D</sub> – Axis 3 <sub>S</sub>	1.3831	24	0.1796

439



440

441 Figure 6. Non-metric multidimensional scaling for modern and fossil pollen assemblages  
 442 from La Mancha lagoon. Modern samples in black diamonds showing sample number,  
 443 whereas fossil samples were symbol coded according to the declared legend.

444

445 **5. Discussion**

446 *5.1 Modern sediments of La Mancha coastal lagoon*

447 Palynological composition of modern samples generally reflected the patterns of modern  
 448 vegetation, incorporating vegetation elements from the surrounding mangroves and salt  
 449 marshes (local vegetation), and nearby lowlands and highland forest (regional vegetation).

450 Although the mangroves of La Mancha are dominated by *A. germinans* over *R. mangle*

451 (Moreno-Casasola, 2006), modern pollen spectra were dominated by the latter (Fig. 3).

452 Given its pollination mechanism, *R. mangle* produces high amounts of pollen, dominating  
453 most of pollen spectra from mangrove forests. Contrastingly, *A. germinans* is an insect-  
454 pollinated species that produces low amounts of pollen (Hogarth, 2007), resulting in under-  
455 representation of the parental taxon in the pollen spectra where percentages as low as 5%  
456 implying an important share in the standing vegetation. However, the mean representation  
457 of *R. mangle* in modern samples from the densely mangrove-forested southern sub-basin  
458 (~25%) are low as compared to pollen spectra from stands dominated by this species which  
459 have been reported as high as 65% (e.g. Behling et al., 2001; Urrego et al., 2009). Although  
460 *C. erecta* and *L. racemosa* are components of the standing forest of La Mancha, they are  
461 not represented in the modern pollen spectra probably because of their low production, and  
462 also because of their distal position with respect to the sampled water body (Moreno-  
463 Casasola, 2006).

464 In the southern sub-basin of La Mancha, the high percentages of *Rhizophora* reflect  
465 the relatively good conservation state of the mangroves (Moreno-Casasola, 2006), with the  
466 exclusive presence of taxa such as *Desmodium*, *Inga* and *Protium* indicating a well  
467 preserved lowland vegetation as well (Franco-Gaviria et al., 2018). Pollen spectra from the  
468 northern sub-basin contained lower percentages of *Rhizophora*, and a substantial  
469 representation of regional pollen, possibly coming from the highlands of the catchment  
470 basin. Over recent decades, the deleterious effects of human activities on mangrove cover  
471 have been more intense around the northern sub-basin of La Mancha lagoon (Lopez-  
472 Portillo et al., 2011; Moreno-Casasola, 2006), reflecting on pollen assemblages where the  
473 regional and disturbance elements are better represented (mainly Moraceae-Urticaceae,  
474 *Myrica*, *Pinus*, Poaceae, and *Quercus*) (Correa-Metrio et al., 2011; Franco-Gaviria et al.,

475 2018). Although *Rhizophora*, Moraceae-Urticaceae, *Pinus*, and *Quercus* do not dominate  
476 the shore vegetation of the most disturbed northern areas, they are represented by pollen  
477 percentages above 10 % each (Fig. 3), reflecting the sparse nature of mangrove forests over  
478 this area. This finding reflects the widely reported overrepresentation of these taxa in pollen  
479 spectra, derived from their high production of pollen and their long-distance pollen  
480 dispersal capacity, as reported for species of anemophyllous pollination (e.g. Correa-Metrio  
481 et al., 2013; Ellison, 2008; Hooghiemstra et al., 2006; Marchant et al., 2002).

482 Modern samples were clustered in the NMDS (Fig. 5), implying more consistency  
483 among the modern pollen spectra than between modern and fossil samples. This finding  
484 demonstrates that the modern heterogeneity of the lagoon does not represent the ecological  
485 and environmental variability of the area over the last ~7800 years. Statistically significant  
486 differences between the NMDS Axis 1 scores of pollen assemblages from the two sub-  
487 basins demonstrate that density of mangrove forest cover can be identified through their  
488 pollen spectra. Overall, these findings indicate that i) pollen assemblages of La Mancha  
489 lagoon are systematically associated with physical and biological attributes of the region at  
490 a broad scale (regional vegetation), and ii) pollen spectra are highly sensitive to the modern  
491 environmental variability throughout La Mancha lagoon (local vegetation). Thus, as  
492 reported for other areas (e.g. Franco-Gaviria et al., 2018; Urrego et al., 2009; Urrego et al.,  
493 2010), modern pollen assemblages of our studied lagoon provide a robust framework for  
494 interpreting our fossil pollen sequence.

495 Higher concentrations of TOC and TN in the southern sub-basin were probably a  
496 result of differences in surrounding vegetation and energy of the depositional environment.  
497 More vigorous vegetation in the southern sub-basin would produce higher amounts of

498 organic matter rich in TOC and TN, whereas the lower energy of the depositional  
499 environment would prevent resuspension and, therefore, further oxidation of the sediments  
500 (Meyers, 1997). Differently, TIC resulted higher in the northern sub-basin, probably  
501 reflecting both higher contribution of marine particulate suspended matter and more  
502 oxidation of organic components (Bouillon et al., 2003). Overall, C and N analyses are  
503 consistent with higher organic matter storage in the sediments of the lagoon where  
504 mangrove forests are well preserved. The relationships that were found between the  
505 different components of C and N demonstrate that in the modern setting of La Mancha,  
506 TOC is the main component of TC. Although these relationships cannot be extrapolated to  
507 the fossil record, they demonstrate that TN is a good proxy for organic matter, and  
508 therefore it is used to offer further support to our pollen-based reconstruction of past  
509 environmental dynamics.

510

## 511 *5.2 Vegetation history of La Mancha Lagoon*

512 The pollen record of La Mancha lagoon reflects the complexities associated with the  
513 multiple factors that have intervened in the development toward the modern biotic and  
514 abiotic systems. Whereas highly variable abundances of regional vegetation suggest  
515 variability in freshwater input by precipitation and tributaries to the lagoon system, pollen  
516 from mangroves together with herbaceous vegetation offer insights into the successional  
517 patterns and development of the local vegetation (Urrego et al., 2013; Urrego et al., 2018).  
518 Additionally, the constant presence of marine shells through the sedimentary record (Fig. 2)  
519 demonstrates a permanent marine influence through the last ~7,800 year. Together, these  
520 indicators illustrate the intimate interaction between sea levels and regional fresh water

521 inputs (precipitation, sediments) that ultimately regulates the colonization, establishment,  
522 and development of mangrove ecosystems in the area. According to our pollen and  
523 geochemical data, the history of the vegetation that surrounds the lagoon and therefore the  
524 regional environmental history could be summarized in four main stages that will be  
525 discussed below.

526 *From c.7800 to 6300 cal BP: sea-water flooding of valleys*

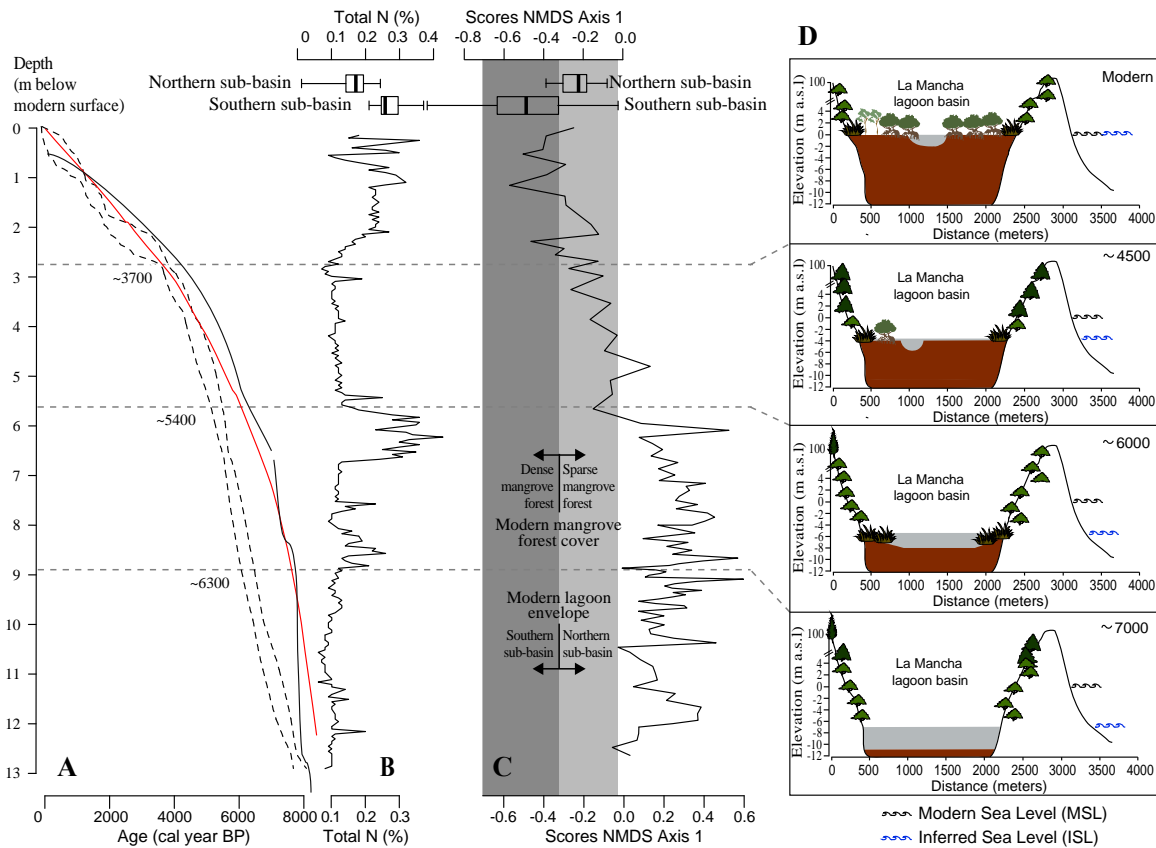
527 Through this time period, the mud-water interface was between 13 and 9 m below the  
528 modern surface, which today is at sea level. At the same time, average sea level was  
529 between 9 and 5 m below modern. The difference between mud-water interface depth and  
530 sea level can only be accounted by lagoon water depth, which was ~ 4 m below sea level  
531 (Fig. 6A). La Mancha Hill, an andesitic rock of Neogene origin (Moreno-Casasola, 2006;  
532 Geissert Kientz, 1999) (Fig. 1), probably acted as a barrier that protected the depositional  
533 environment from the erosive energy of the waves and winds. Through this period, even  
534 though sedimentation rates at La Mancha (~3.04 mm/year) were lower than the inferred  
535 rate of sea-level increase, they are among the highest through the record. High rates of both  
536 regional sea-level rise and sedimentation at La Mancha are likely a result of the regional  
537 geologic instability that characterized the conformation of the modern Gulf of Mexico in its  
538 final stages, up to 5000 cal BP (Davis, 2011). As sea level increased through the  
539 deglaciation and the early Holocene, sea-water flooded coastal plains and valleys at a speed  
540 that surpassed the accumulation of continental sediments. Thus, the lacustrine basin of La  
541 Mancha was probably deeper than modern, impeding the establishment of mangrove forests  
542 (Fig. 6C). A peak of *Rhizophora* from the bottom of the record to ~7500 cal BP (Fig. 4)  
543 probably shows the colonization of mangroves during the initial stages of the lagoon and



544 the sea-water flooding, which were subsequently displaced by the formation of a deep-  
545 water body.

546 In México, *Pinus* populations thrive under early post-disturbance successional  
547 stages, or under conditions that are not optimal for other taxa (Metcalfé et al., 2000;  
548 Ramírez-Marcial et al., 2001). Thus, the persistence of *Pinus* in high percentages from the  
549 bottom of the record to ~6500 cal BP (Fig. 5) indicates that regional conditions were likely  
550 dry, an interpretation that is further supported by the lowest concentrations of TN (Fig. 7)  
551 and therefore of organic matter. These dry conditions probably played a central role at  
552 maintaining sedimentation rates that did not offset sea-level rise, impeding the  
553 establishment of mangrove forests, as demonstrated by the NMDS Axis 1 scores that were  
554 outside the envelope defined by modern samples (Fig. 7C).

555



556

557 Figure 7. Environmental history of La Mancha Lagoon through the last 7,800 years. **A.**  
 558 Age-depth model of core MAN15V from La Mancha Lagoon (dashed lines show 95%  
 559 confidence interval), compared with sea level rise curves for the Caribbean (red line,  
 560 Toscano and Macintyre, 2003) and the northern Gulf of Mexico (black solid line, Milliken  
 561 and Anderson, 2008). **B.** Sedimentary total nitrogen content (%); boxplots illustrate total  
 562 nitrogen in modern samples from the northern (up) and southern (down) sub-basins of the  
 563 lagoon (whiskers show minimum and maximum scores). **C.** NMDS Axis 1 scores through  
 564 time; boxplots illustrate scores of modern samples; scores of the modern environmental  
 565 envelope represented by modern samples are highlighted in grey; scores of the interquartile  
 566 range of samples from the well preserved southern sub-basin are in dark grey. **D.** Schematic  
 567 development of La Mancha Lagoon, illustrated at ~7,000, 6000, 4,500 cal BP, and Modern.

568

569 *From c. 6300 to 5400 cal BP: development of lagoon shores*

570 Whereas the rate of sea-level rise started to decline through this period, sedimentation rates  
571 at La Mancha remained high (3.86 mm/yr, Fig. 6). This phenomenon could be explained by  
572 two critical factors: i) following the reported deceleration of sea-level rise at ~7000 cal BP  
573 (Toscano and Macintyre, 2003), sand bars started accumulating at the mouth of coastal  
574 lagoons (Davis, 2011), providing a more stable plain for sediment accumulation at La  
575 Mancha; and ii) a substantial decrease in the percentages of *Pinus*, and an increase of  
576 montane forest taxa (e.g. *Alnus*, *Quercus*, and *Ulmaceae*) indicate wetter conditions that  
577 would be in turn associated with higher river sediment discharge. These regional wetter  
578 conditions could be related to the final stages of the Holocene Thermal Maximum, which  
579 was in general characterized by higher than present precipitation and temperature in the  
580 Northern Hemisphere (Renssen et al., 2009).

581         The lagoon became shallower, and the development of muddy shores is evidenced  
582 by high percentages of salt marsh vegetation (Fig. 5), and high accumulation of organic  
583 matter revealed by the increasing TN (Fig. 7B). This state of local vegetation and the high  
584 accumulation of organic matter suggest the closing of the ephemeral mouth, probably  
585 caused by lower energy associated with the shallowing of the lagoon, together with the  
586 intensification of the wind currents, and sea level changes reported for the Gulf of Mexico  
587 and the Caribbean (Balsille and Donoghue, 2004; González and Dupont, 2009; Urrego et  
588 al., 2013; Wooller et al., 2007). Pollen spectra suggest the early stages of a successional  
589 pattern of mangrove vegetation associated with the marine transgression, although NMDS

590 Axis 1 sample scores demonstrate that mangrove forests were not established yet near the  
591 location where the core was retrieved.

592 *From c. 5400 to 3700 BP: A regional drought*

593 Whereas the rate of sea-level rise continued to decrease, relatively high sedimentation rates  
594 were evident in La Mancha sequence up to ~5000 cal BP, when apparently the rates of  
595 sediment deposition in the lagoon and those of sea level rise became similar (Fig. 6A).  
596 Such equilibrium between sediment deposition and sea-level rise implies the definition of a  
597 coastal erosive baseline that allowed the deposition of sand in the coast by the northerly  
598 currents during the dry season, creating the sandbar that dams the lagoon. Differently,  
599 during the wet season, the fluvial input would have the capacity to erode the sandbar,  
600 opening the direct contact between the lagoon and the sea and, thus, resulting in the modern  
601 seasonal flood cycle. During the dry season, the coastal bar would be closed by the action  
602 of the waves and the prevailing winds, whereas during the rainy season the bar would be  
603 opened by the energy of the fresh water discharge. The lagoon thus became a shallow water  
604 body ( $z_{\max} \sim 1$  m) mostly protected from the energy of the waves by La Mancha hill (Fig.1),  
605 and subjected to seasonal tidal and climatic fluctuations.

606 From c. 5400 to 3700 cal BP, the recurrent drainage of fresh water into the sea  
607 probably created a series of channels giving the lagoon a physiography very similar to  
608 modern. However, according to the NMDS scores, vegetation at that time resembled the  
609 northern sub-basin today (Fig. 6B), an area characterized by poorly developed sparse  
610 mangrove stands. Thus, vegetation assemblages from this period were a result of  
611 suboptimal environmental conditions for mangrove forest development. High percentages  
612 of *Pinus* (up to 60%) through this period suggest that there was a regional drought in place,

613 which likely maintained high substrate salinity by reducing freshwater river discharge to  
614 the lagoon. Thus, local vegetation consisted of a mixture of sparse mangrove trees with  
615 some salt marshes species, and a slow increase of mangrove pollen because of the  
616 prevailing dry conditions (Fig. 4). Although anthropogenic influence cannot be discarded as  
617 a plausible explanation for the sparse mangrove vegetation, the inference of a regional  
618 drought is supported by similar reports from Lake Petén Itzá between ~ 4500 up to ~3000  
619 cal BP, Lake Tzib (Quintana Roo) at ~3500 cal BP (Carrillo-Bastos et al., 2010; Mueller et  
620 al., 2010), and also in the Cariaco Basin record, with a trend from ~5400 up to the present  
621 (Haug et al., 2001). Furthermore, the abrupt decrease of TN and its linear trend towards  
622 even lower concentrations (Fig. 7B) evidence rather oxidizing conditions, an environmental  
623 process that is difficult to explain from the perspective of human occupation.

624

625 *From c. 3700 cal BP to Present: the establishment of modern mangrove forests*

626 Mangrove pollen taxa showed the highest percentages (Fig. 5), reflecting an environment of  
627 relative stability where the exchange of saline and fresh water, and the input of sediments  
628 were balanced, producing an increase of mangrove forest biomass (Krauss et al., 2008).

629 These conditions provided consolidated clay sediments, where as indicated by the NMDS  
630 scores, mangrove forests developed into mature forest stands of *Rhizophora* and *Avicennia*.

631 Increasing concentrations of TN (Fig. 7B) indicate high accumulation of organic matter  
632 probably associated with the establishment of the mangrove forest (Bouillon et al. 2003).

633 Sea level continued to increase at slower rates (Balsille and Donoghue, 2004) that were  
634 matched by the rate of sediment accumulation in La Mancha (~0.92 mm/yr on average).

635 These more stable conditions for coastal ecosystems have been reported for other localities

636 in the Caribbean coinciding with other records (Urrego et al., 2013), where mangrove  
637 forests developed under a relatively stable sedimentation rate (1.09 to 0.89 mm/yr).

638 *Pinus* and salt marsh pollen in La Mancha showed substantial decreases caused by  
639 wetter conditions and higher representation of local mangrove pollen, implying a lower  
640 regional influence on pollen spectra, and the continuation of the successional processes that  
641 led to the establishment of the mangrove forest (González and Dupont, 2009). At this stage,  
642 the lagoon seems to have reached its modern configuration, with influences from local  
643 processes like the annual opening of the ephemeral mouth, fluctuating floods of salt water,  
644 input of fresh water from the streams, and anthropogenic activities (Moreno-Casasola,  
645 2006). Indeed, the sharp decrease of *Rhizophora* is likely reflecting the terrestrialization of  
646 the cored site, which today is occupied by an *Avicennia germinans* forest that floods only  
647 when the ephemeral mouth is closed and the lagoon reaches its maximum water level  
648 through the year. This latter observation is further supported by the high variability of TN  
649 concentrations towards the top of the record.

650

## 651 **6. Conclusion**

652 The sedimentary record of La Mancha lagoon encompasses the history of local and regional  
653 environmental conditions through the last ~8,000 years, including the establishment of  
654 modern mangrove forest along the coast of Veracruz. The record shows the regional  
655 context under which the coastal lagoon formed, showing the transformation of the lagoon  
656 from a water body with permanent communication with the sea to the modern seasonally  
657 closed system. When sea level rise rates were higher than the rates of sediment infill of the  
658 lagoon's basin, the depositional environment was under sea level and pollen assemblages

659 were dominated by regional taxa. The ecological succession towards the establishment of  
660 mangrove forest started at ~6,300 cal BP, but mangrove forests were sparse, resembling  
661 those of the modern northern sub-basin because of two main reasons: i) the water column  
662 was relatively deep and sedimentary plains for mangrove establishment were likely narrow,  
663 and ii) a regional drought lasting from ~5400 to 3700 BP probably caused extremely high  
664 substrate salinity that impeded mangrove forests expansion. Dense mangrove forests like  
665 those that occupy the southern sub-basin today established around ~3500 BP, and have  
666 dominated the area ever since.

667         The matching of lagoon sediment and sea levels at ~4000 cal BP was likely  
668 associated with the development of the seasonally open mouth. This pairing of lagoon  
669 sedimentary accumulation and sea levels defined the latter as the base level for erosion,  
670 allowing the accumulation of material during the dry season, and therefore the formation of  
671 a damming bar, which would eventually be open during the rainy season owing to the  
672 increased freshwater discharge. Concomitant to this process would be the linear erosion of  
673 channels through the sedimentary deposit, conforming the modern geomorphology of the  
674 area. The establishment of the mangrove forest implied a substantial increase of  
675 sedimentary organic matter, highlighting the role of these ecosystems at storing carbon.  
676 Overall, our record demonstrates the complexity of the interactions between local and  
677 regional factors in the development and evolution of both coastal geomorphology and  
678 ecosystems.

679

680 **Acknowledgements**

681

682 This research was funded by Programa de Apoyo a Proyectos de Investigación e  
683 Innovación Tecnológica PAPIIT-UNAM [grant number IN107716], and Consejo Nacional  
684 de Ciencia y Tecnología [grant number 256406]. Alex Correa-Metrio was supported by  
685 Programa de Apoyos para la Superación del Personal Académico de la UNAM (PASPA).  
686 Dayenari Caballero-Rodríguez, Esmeralda Cruz Silva, Roberto Maya Hernández, and  
687 Yosahandy Vázquez Molina are thanked for their assistance in the field.

688

## 689 **7. References**

- 690 Ball, M.C., 2002. Interactive effects of salinity and irradiance on growth: implications for mangrove  
691 forest structure along salinity gradients. *Trees*, 16, 126-139.
- 692 Balsillie, J.H., Donoghue, J.F., 2004. High resolution sea-level history for the Gulf of Mexico since  
693 the last glacial maximum. Florida Geological Survey.
- 694 Behling, H., Cohen, M.C.L., Lara, R.J., 2001. Studies on Holocene mangrove ecosystems dynamics  
695 of the Braganca Peninsula in north-eastern Para, Brazil. *Palaeogeography,*  
696 *Palaeoclimatology, Palaeoecology*, 167, 225-242.
- 697 Blaauw, M., Christen, J.A., 2011. Flexible paleoclimate age-depth models using an autoregressive  
698 gamma process. *Bayesian Analysis*, 6, 457-474.
- 699 Bouillon, S. et al., 2008. Mangrove production and carbon sinks: a revision of global budget  
700 estimates. *Global Biogeochemical Cycles*, 22.
- 701 Bouillon, S., Dahdouh-Guebas, F., Rao, A., Koedam, N., Dehairs, F., 2003. Sources of organic carbon  
702 in mangrove sediments: variability and possible ecological implications. *Hydrobiologia*,  
703 495, 33-39.
- 704 Bush, M.B., 2002. On the interpretation of fossil Poaceae pollen in the lowland humid neotropics.  
705 *Palaeogeography, Palaeoclimatology, Palaeoecology*, 177, 5-17.
- 706 Carrillo-Bastos, A., Islebe, G.A., Torrescano-Valle, N., González, N.E., 2010. Holocene vegetation  
707 and climate history of central Quintana Roo, Yucatan Peninsula, Mexico. *Review of*  
708 *Palaeobotany & Palynology*, 160, 189-196.
- 709 Colinvaux, P., de Olivera, P.E., Moreno, P.J.E., 1999. *Amazon Pollen Manual and Atlas*. Harwood  
710 Academic Publishers, Amsterdam.
- 711 Correa-Metrio, A., Bush, M.B., Lozano-García, M.S., Sosa-Nájera, S., 2013. Millennial-scale  
712 temperature change velocity in the continental northern Neotropics. *PLoS ONE*, 8, e81958.
- 713 Correa-Metrio, A., Bush, M.B., Pérez, L., Schwalb, A., Cabrera, K.R., 2011. Pollen distribution along  
714 climatic and biogeographic gradients in northern Central America. *The Holocene*, 21, 681-  
715 692.
- 716 Davis, R.A., 2011. *Sea-level change in the Gulf of Mexico*. Texas A&M University Press, Corpus  
717 Christi.
- 718 Ellison, J.C., 1989. Pollen analysis of mangrove sediments as a sea-level indicator: assessment from  
719 Tongatapu, Tonga. *Palaeogeography, Palaeoclimatology, Palaeoecology*, 74, 327-341.



720 Ellison, J.C., 2008. Long-term retrospection on mangrove development using sediment cores and  
721 pollen analysis: a review. *Aquatic Botany*, 89, 93-104.

722 Faegri, K., Iversen, J., 1989. Textbook of pollen analysis. 4th ed. Wiley, Chichester.

723 Faith, D.P., Minchin, P.R., Belbin, L., 1987. Compositional dissimilarity as a robust measure of  
724 ecological distance. *Vegetatio*, 69, 57-68.

725 FAO-UNEP, 2007. The world's mangroves 1980–2005. FAO Forestry Paper.

726 Feller, I.C., Friess, D.A., Krauss, K.W., Lewis, R.R., 2017. The state of the world's mangroves in the  
727 21st century under climate change. *Hydrobiologia*, 803, 1-12.

728 Franco-Gaviria, F. et al., 2018. The human impact imprint on the modern pollen spectra of the  
729 Maya lands. *Boletín de la Sociedad Geológica Mexicana*, 70, 61-78.

730 Geissert Kientz, D., 1999. Regionalización geomorfológica del estado de Veracruz. *Investigaciones  
731 geográficas*, 23-47.

732 Gilman, E.L., Ellison, J., Duke, N.C., Field, C., 2008. Threats to mangroves from climate change and  
733 adaptation options: a review. *Aquatic botany*, 89, 237-250.

734 González, C., Dupont, L.M., 2009. Tropical salt marsh succession as sea-level indicator during  
735 Heinrich events. *Quaternary Science Reviews*, 28, 939-946.

736 González, C., Urrego, L.E., Martínez, J.I., Polanía, J., Yokoyama, Y., 2010. Mangrove dynamics in the  
737 southwestern Caribbean since the 'Little Ice Age': A history of human and natural  
738 disturbances. *The Holocene*, 20, 849-861.

739 Hamilton, S.E., Casey, D., 2016. Creation of a high spatio-temporal resolution global database of  
740 continuous mangrove forest cover for the 21st century (CGMFC-21). *Global Ecology and  
741 Biogeography*, 25, 729-738.

742 Haug, G.H., Hughen, K.A., Sigman, D.M., Peterson, L.C., Rohl, U., 2001. Southward migration of the  
743 Intertropical Convergence Zone through the Holocene. *Science*, 293, 1304-1308.

744 Hogarth, P.J., 2015. The biology of mangroves and seagrasses. Oxford University Press, Oxford.

745 Hooghiemstra, H., Lézine, A.M., Leroy, S.A.G., Dupont, L., Marret, F., 2006. Late Quaternary  
746 palynology in marine sediments: A synthesis of the understanding of pollen distribution  
747 patterns in the NW African setting. *Quaternary International*, 148, 29-44.

748 Kjerfve, B., 1994. Coastal lagoon processes. Elsevier, Amsterdam.

749 Krauss, K.W. et al., 2008. Environmental drivers in mangrove establishment and early  
750 development: a review. *Aquatic Botany*, 89, 105-127.

751 Lankford, R.R., 1977. Coastal lagoons of Mexico their origin and classification, *Estuarine Processes:  
752 Circulation, Sediments, and Transfer of Material in the Estuary*. Elsevier, pp. 182-215.

753 Legendre, P., Legendre, L., 2012. Numerical Ecology. Elsevier Scientific, Oxford.

754 López-Portillo, J., 2011. Atlas de las costas de Veracruz: manglares y dunas [costeras]. Gobierno del  
755 Estado de Veracruz, Secretaría de Educación, Xalapa.

756 Lugo, A.E., Snedaker, S.C., 1974. The ecology of mangroves. *Annual review of ecology and  
757 systematics*, 5, 39-64.

758 Marchant, R. et al., 2002. Distribution and ecology of parent taxa of pollen lodged within the Latin  
759 American Pollen Database. *Review of Palaeobotany and Palynology*, 121, 1-75.

760 Méndez Linares, A., López-Portillo, J., Hernández-Santana, J., Pérez, M.O., Orozco, O.O.J.C., 2007.  
761 The mangrove communities in the Arroyo Seco deltaic fan, Jalisco, Mexico, and their  
762 relation with the geomorphic and physical–geographic zonation. *70*, 127-142.

763 Metcalfe, S.E., O'Hara, S.L., Caballero, M., Davies, S.J., 2000. Records of Late Pleistocene-Holocene  
764 climate change in Mexico- a review. *Quaternary Science Reviews*, 19, 699-721.

765 Meyers, P.A., 1997. Organic geochemical proxies of paleoceanographic, paleolimnologic, and  
766 paleoclimatic processes. *Organic geochemistry*, 27, 213-250.

767 Milliken, K., Anderson, J.B., Rodriguez, A.B., 2008. A new composite Holocene sea-level curve for  
768 the northern Gulf of Mexico. *Geological Society of America Special Paper*, 443, 1-11.

769 Moreno-Casasola, P., 2006. *Entornos veracruzanos: la costa de La Mancha*, Instituto de Ecología,  
770 A.C., Xalapa, Veracruz, Mexico.

771 Mueller, A.D. et al., 2010. Late Quaternary palaeoenvironment of northern Guatemala: evidence  
772 from deep drill cores and seismic stratigraphy of Lake Petén Itzá. *Sedimentology*, 57, 1220-  
773 1245.

774 Parkinson, R.W., DeLaune, R.D., White, J.R., 1994. Holocene sea-level rise and the fate of  
775 mangrove forests within the wider Caribbean region. *Journal of Coastal Research*, 1077-  
776 1086.

777 Ramírez-Marcial, N., González-Espinosa, M., Williams-Linera, G., 2001. Anthropogenic disturbance  
778 and tree diversity in montane rain forests in Chiapas, Mexico. *Forest Ecology  
779 Management*, 154, 311-326.

780 Ranwell, D.S., 1972. Ecology of salt marshes and sand dunes, *Ecology of salt marshes and sand  
781 dunes*. Chapman and Hall, London, pp. 200 pp.

782 Reimer, P.J. et al., 2013. IntCal13 and Marine13 radiocarbon age calibration curves 0–50,000 years  
783 cal BP. *Radiocarbon*, 55, 1869-1887.

784 Renssen, H. et al., 2009. The spatial and temporal complexity of the Holocene thermal maximum.  
785 *Nature Geoscience*, 2, 411-414.

786 Richardson, D.M., 1998. *Ecology and Biogeography of Pinus*. Cambridge University Press,  
787 Cambridge.

788 Rzedowski, J., 2006. *Vegetación de México*. Comisión Nacional para el Conocimiento y Uso de la  
789 Biodiversidad, México D.F., pp. 504 pp.

790 Servicio Meteorológico Nacional, 2018. Normales climatológicas, Estado de Veracruz, Estación La  
791 Mancha (online, last accessed June 2018).

792 Soares, M., 2009. A conceptual model for the responses of mangrove forests to sea level rise.  
793 *Journal of Coastal Research*, 267-271.

794 Suárez, J.A., Urrego, L.E., Osorio, A., Ruiz, H.Y., 2015. Oceanic and climatic drivers of mangrove  
795 changes in the Gulf of Urabá, Colombian Caribbean. *Latin American Journal of Aquatic  
796 Research*, 43.

797 Thom, B.G., 1967. Mangrove ecology and deltaic geomorphology: Tabasco, Mexico. *The Journal of  
798 Ecology*, 301-343.

799 Thorhaug, A., Poulos, H.M., López-Portillo, J., Ku, T.C., Berlyn, G., 2017. Seagrass blue carbon  
800 dynamics in the Gulf of Mexico: Stocks, losses from anthropogenic disturbance, and gains  
801 through seagrass restoration. *Science of The Total Environment*, 605, 626-636.

802 Toscano, M.A., Macintyre, I.G., 2003. Corrected western Atlantic sea-level curve for the last 11,000  
803 years based on calibrated 14C dates from *Acropora palmata* framework and intertidal  
804 mangrove peat. *Coral reefs*, 22, 257-270.

805 Travieso-Bello, A., 2000. *Biodiversidad del paisaje costero de La Mancha*, Actopan, Veracruz.  
806 Instituto de Ecología, Xalapa.

807 Urrego, L.E., Bernal, G., Polanía, J., 2009. Comparison of pollen distribution patterns in surface  
808 sediments of a Colombian Caribbean mangrove with geomorphology and vegetation.  
809 *Review of Palaeobotany and Palynology*, 156, 358-375.

810 Urrego, L.E., Correa-Metrio, A., González, C., Castaño, A.R., Yokoyama, Y., 2013. Contrasting  
811 responses of two Caribbean mangroves to sea-level rise in the Guajira Peninsula  
812 (Colombian Caribbean). *Palaeogeography, Palaeoclimatology, Palaeoecology*, 370, 92-102.

813 Urrego, L.E., Correa-Metrio, A., González-Arango, C., 2018. Colombian Caribbean mangrove  
814 dynamics: anthropogenic and environmental drivers. *Boletín de la Sociedad Geológica*  
815 *Mexicana*, 70, 133-145.

816 Urrego, L.E., González, C., Urán, G., Polanía, J., 2010. Modern pollen rain in mangroves from San  
817 Andres Island, Colombian Caribbean. *Review of Palaeobotany and Palynology*, 162, 168-  
818 182.

819 Valiela, I., Bowen, J.L., York, J.K., 2001. Mangrove Forests: One of the World's Threatened Major  
820 Tropical Environments. *Bioscience*, 51, 807-815.

821 Vovides, A.G. et al., 2014. Morphological plasticity in mangrove trees: salinity-related changes in  
822 the allometry of *Avicennia germinans*. *Trees*, 28, 1413-1425.

823 Ward, R.D., Friess, D.A., Day, R.H., MacKenzie, R.A., 2016. Impacts of climate change on mangrove  
824 ecosystems: a region by region overview. *Ecosystem Health Sustainability*, 2, e01211.

825 Williams-Linera, G., 2002. Tree species richness complementarity, disturbance and fragmentation  
826 in a Mexican tropical montane cloud forest. *Biodiversity & Conservation*, 11, 1825-1843.

827 Wooller, M.J., Morgan, R., Fowell, S., Behling, H., Fogel, M., 2007. A multiproxy peat record of  
828 Holocene mangrove palaeoecology from Twin Cays, Belize. *The Holocene*, 17, 1129-1139.

829 Zar, J.H., 1999. *Biostatistical Analysis*. 4th ed. Prentice-Hall, Upper Saddle River, NJ.

830

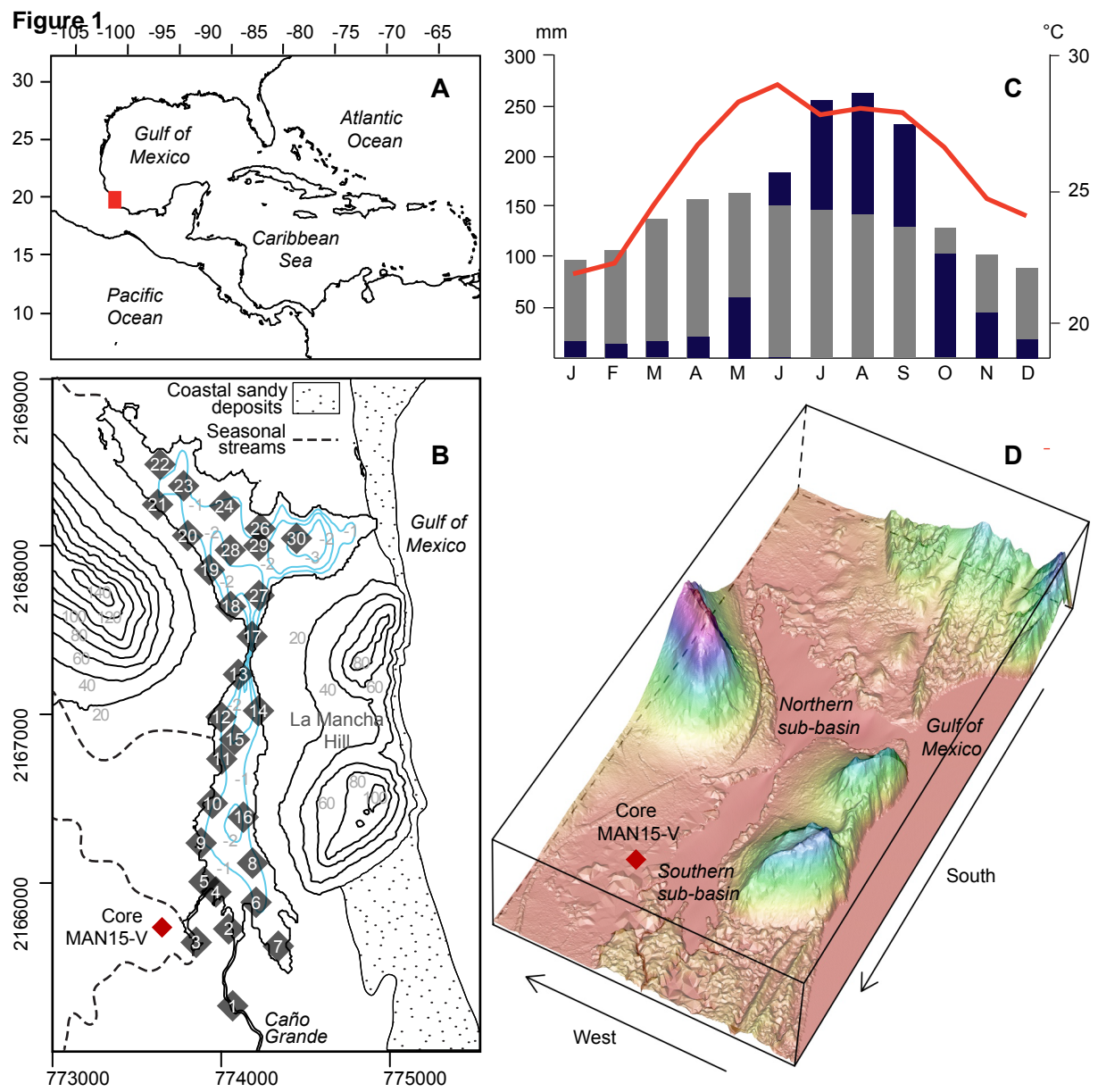
## \*Highlights (for review)

- During the mid Holocene, sedimentation rates were lower than sea level rise rates
- Modern barrier-lagoon systems of the Gulf of Mexico appeared ~5000 years ago
- A drought between 5400 and 3700 years ago impeded mangrove forest establishment
- Modern coastal lagoons of the western Gulf of Mexico established ~3700 years ago
- The establishment of mangroves caused an increase of sedimentary organic matter

**Table 1**[Click here to download Table: Table1.docx](#)

Table 1. Radiocarbon dates of core MAN15V from La Mancha coastal lagoon. Depths in cm below lagoon floor (blf). Ages calibrated after the IntCal13 curve (Reimer et al., 2013).

Laboratory code	Depth (cm blf)	<sup>14</sup> C Age	Error	Calibrated age (95% range; cal BP)
UBA-34340	109	1290	24	1181-1283
Beta-440367	175	1880	30	1730-1883
UBA-34341	282	3447	26	3637-3826
Beta-440368	373	3970	30	4300-4523
UBA-34342	564	4732	41	5326-5584
Beta-437078	649	4770	30	5334-5588
UBA-34343	979	5624	41	6312-6482
Beta-437079	1249	6700	30	7508-7616



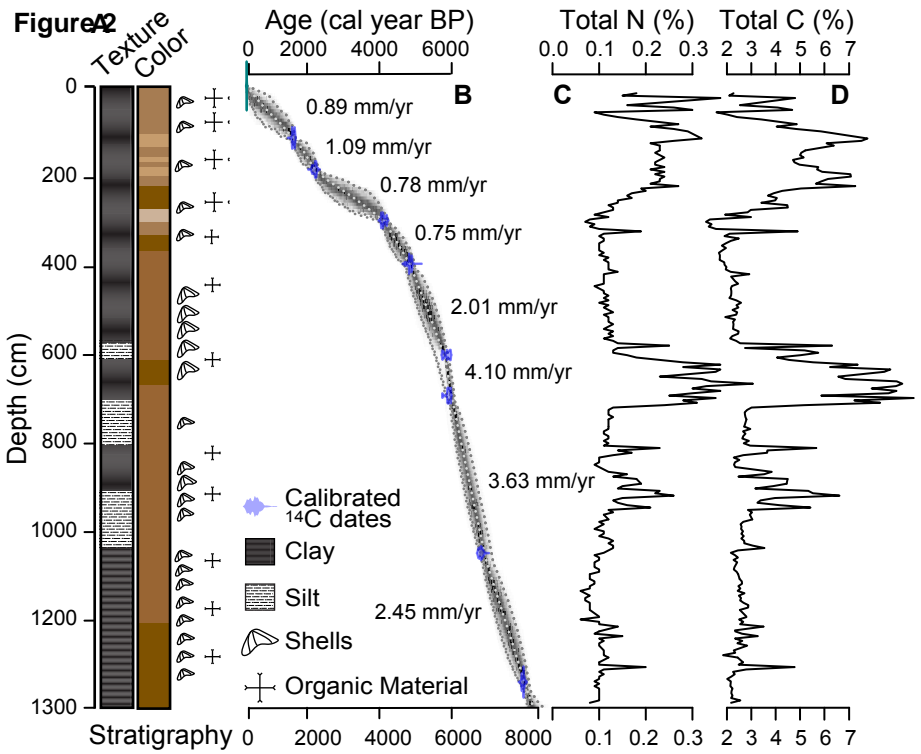
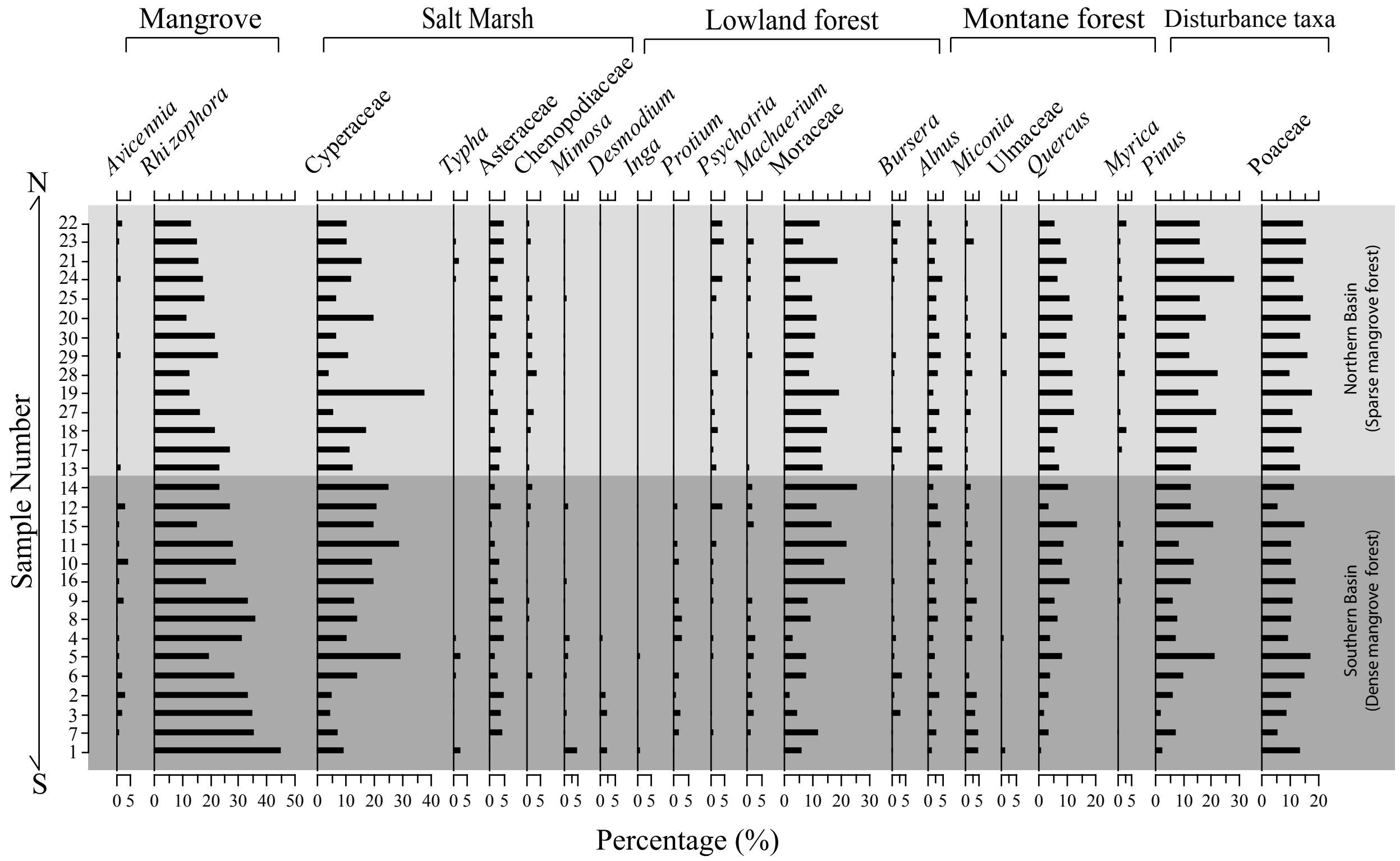
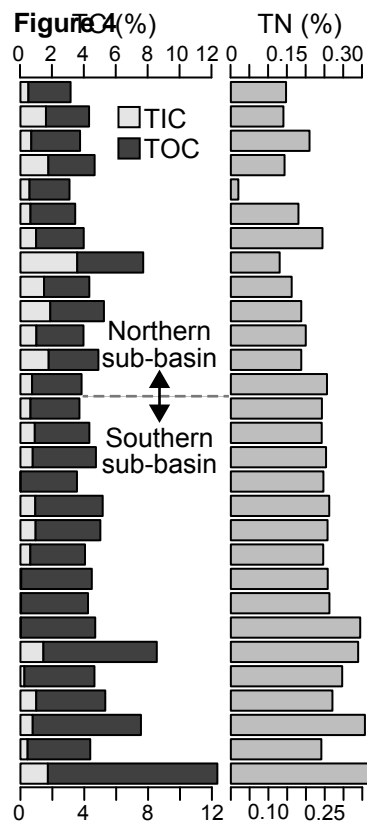


Figure 3







◆ Southern sub-basin    ◆ Northern sub-basin    NS Non significant

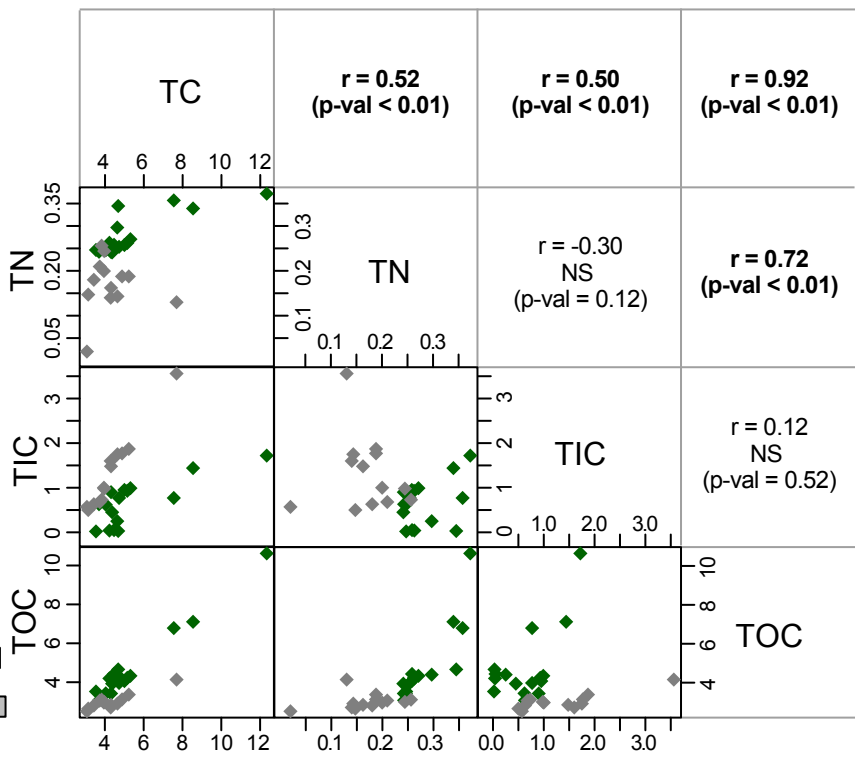


Figure 5

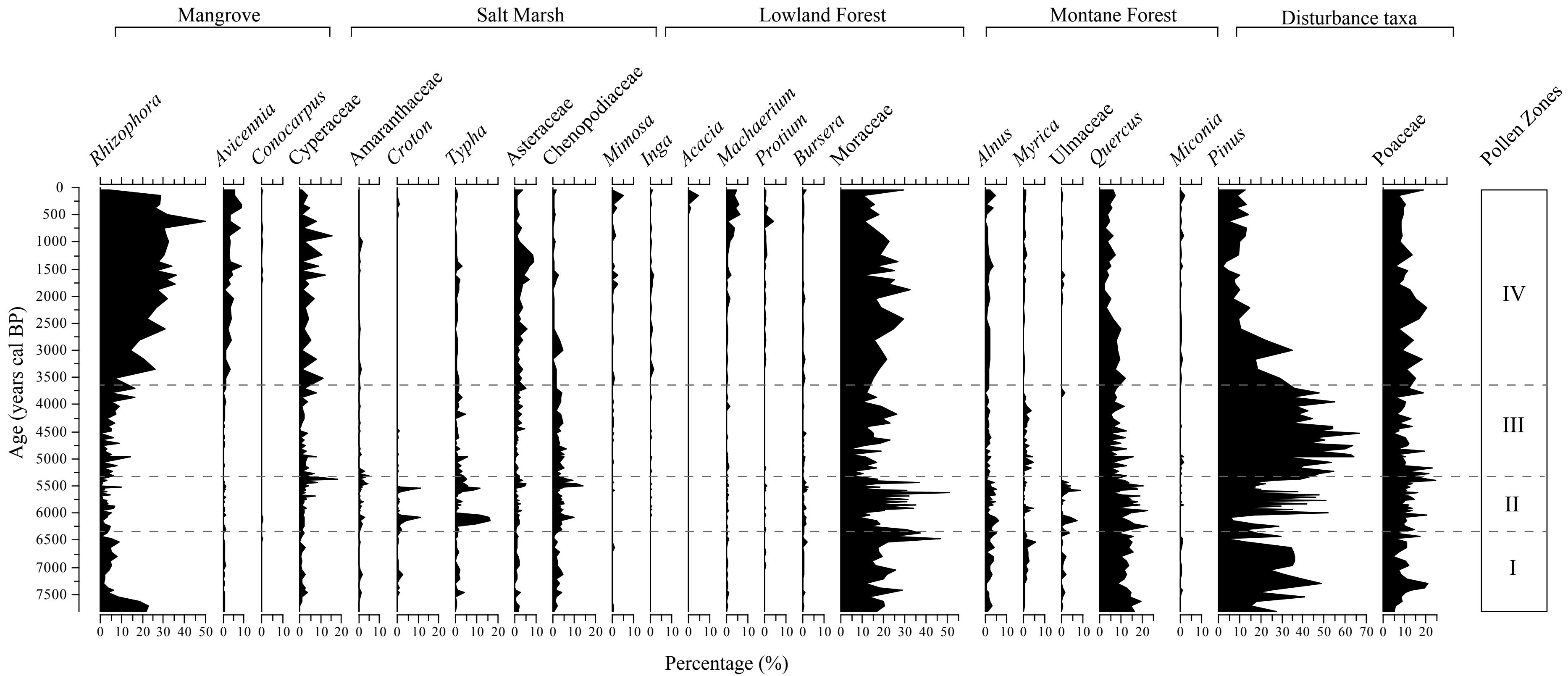
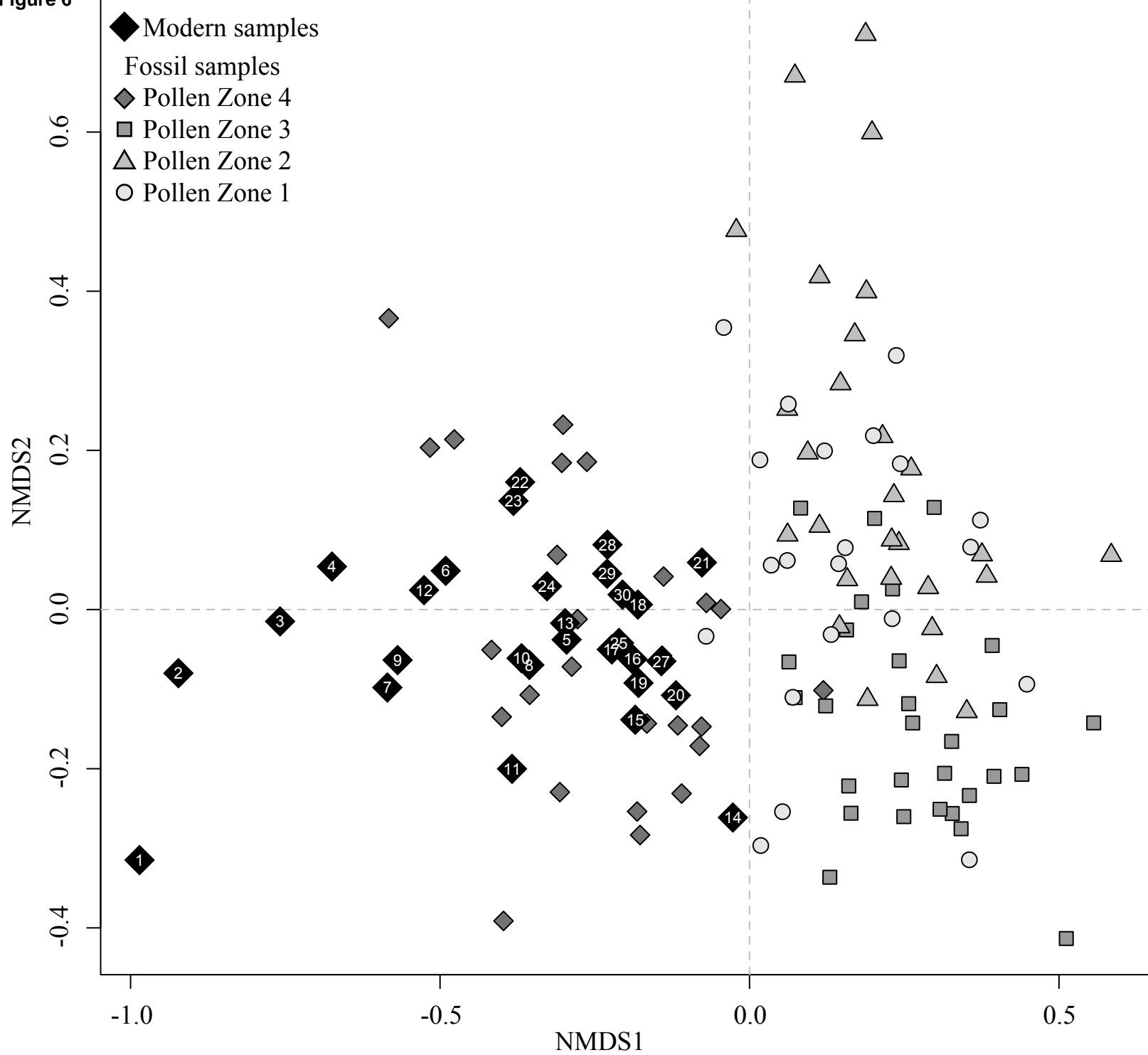


Figure 6



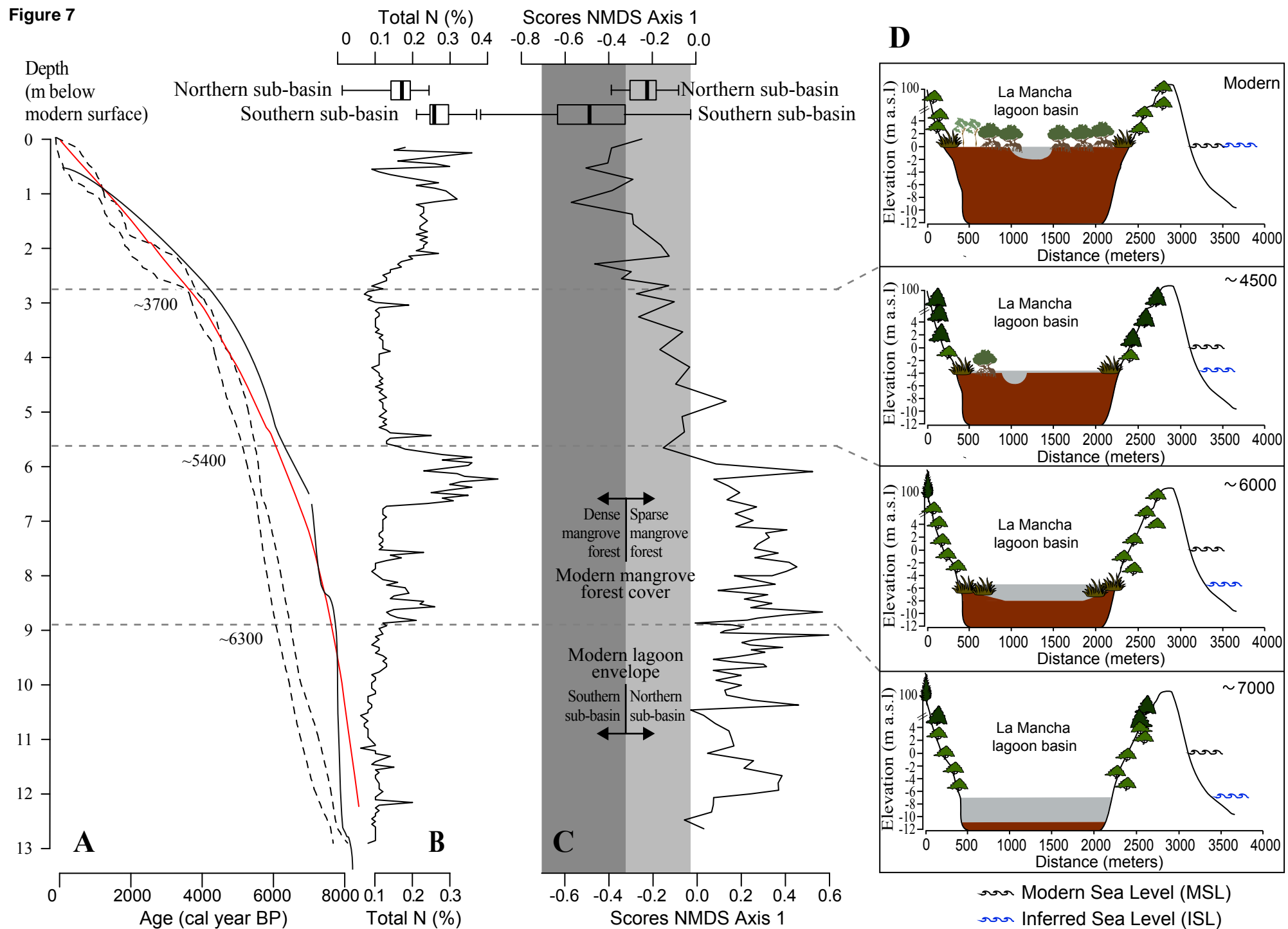
**Figure 7**

Figure 1. Study area. A. Location of La Mancha lagoon in the continental context. B. Locations sampled for modern and fossil sediments in the local context of La Mancha coastal lagoon; elevation contours are shown in increments of 20 m asl (solid black lines), whereas a basic bathymetry based on field observations is shown as blue contours. C. Monthly precipitation (blue bars), evapotranspiration (gray bars), and monthly mean temperature (black line with dots) at La Mancha Meteorological Station (Servicio Meteorológico Nacional, 2018) D. Topographic representation of La Mancha coastal lagoon.

Figure 2. Core MAN15V from La Mancha coastal lagoon. A. Stratigraphy of the sedimentary sequence: texture (left), color (right), and organic and shell content. B. Age-depth model; calibrated ages (blue silhouettes), 95% confidence intervals in grey (darker colors indicate higher probability), and sedimentation rates (mm/yr). C and D. Percentage of total nitrogen and total carbon content (TN and TC, respectively).

Figure 3. Pollen diagram of selected taxa from mud-water interface samples from La Mancha coastal lagoon. Ecological affinities after Lugo and Snedaker (1974), Ramwell (1972), and Travieso-Bello (2000). Samples are ordered from South to North with samples from the southern (northern) sub-basin highlighted in dark (light) grey.

Figure 4. Content (%) of carbon and nitrogen in the modern samples of La Mancha coastal lagoon. Total C content (TC) discriminated into inorganic and organic fractions (TIC and

TOC), and total N content (TN). Comparisons among sedimentary attributes are shown in the right side panels (biplots and correlation coefficients with their significance).

Figure 5. Fossil pollen diagram of selected taxa of core MAN15V from La Mancha coastal lagoon. (ecological affinities after Lugo and Snedaker 1974, Ramwell 1972, and Travieso-Bello 2000).

Figure 6. Non-metric multidimensional scaling for modern and fossil pollen assemblages from La Mancha lagoon. Modern samples in black diamonds showing sample number, whereas fossil samples were symbol coded according to the declared legend.

Figure 7. Environmental history of La Mancha Lagoon through the last 7,800 years. **A.** Age-depth model of core MAN15V from La Mancha Lagoon (dashed lines show 95% confidence interval), compared with sea level rise curves for the Caribbean (red line, Toscano and Macintyre, 2003) and the northern Gulf of Mexico (black solid line, Milliken and Anderson, 2008). **B.** Sedimentary total nitrogen content (%); boxplots illustrate total nitrogen in modern samples from the northern (up) and southern (down) sub-basins of the lagoon (whiskers show minimum and maximum scores). **C.** NMDS Axis 1 scores through time; boxplots illustrate scores of modern samples; scores of the modern environmental envelope represented by modern samples are highlighted in grey; scores of the interquartile range of samples from the well preserved southern sub-basin are in dark grey. **D.** Schematic development of La Mancha Lagoon, illustrated at ~7,000, 6000, 4,500 cal BP, and Modern.

**Supplementary material for on-line publication only**

[Click here to download Supplementary material for on-line publication only: Cordero\\_etal\\_Supplementary material.docx](#)